Received: 22 January 2022 | Revised: 22 June 2022 | Accepted: 4 July 2022

DOI: 10.1111/mec.16604

SPECIAL ISSUE

MOLECULAR ECOLOGY WILEY

Whole-genome phylogeography of the blue-faced honeyeater (*Entomyzon cyanotis*) and discovery and characterization of a neo-Z chromosome

John T. Burley[1,2,3,4] | Sophia C. M. Orzechowski[1] | Simon Yung Wa Sin[1,5] | Scott V. Edwards[1]

[1]Museum of Comparative Zoology, Harvard University, Cambridge, Massachusetts, USA

[2]Department of Evolutionary Biology, Evolutionary Biology Centre (EBC), Uppsala University, Uppsala, Sweden

[3]Department of Ecology Evolution and Organismal Biology, Brown University, Providence, Rhode Island, USA

[4]Institute at Brown for Environment and Society, Brown University, Providence, Rhode Island, USA

[5]School of Biological Sciences, The University of Hong Kong, Hong Kong SAR, China

Correspondence
Scott V. Edwards, Museum of Comparative Zoology, Harvard University, Cambridge, MA 02138, USA.
Email: sedwards@fas.harvard.edu

Funding information
Harvard University; Mundus Erasmus Master for Evolutionary Biology (MEME) programme

Handling Editor: Dan G. Bock

Abstract

Whole-genome surveys of genetic diversity and geographic variation often yield unexpected discoveries of novel structural variation, which long-read DNA sequencing can help clarify. Here, we report on whole-genome phylogeography of a bird exhibiting classic vicariant geographies across Australia and New Guinea, the blue-faced honeyeater (*Entomyzon cyanotis*), and the discovery and characterization of a novel neo-Z chromosome by long-read sequencing. Using short-read genome-wide SNPs, we inferred population divergence events within *E. cyanotis* across the Carpentarian and other biogeographic barriers during the Pleistocene (~0.3–1.7 Ma). Evidence for introgression between nonsister populations supports a hypothesis of reticulate evolution around a triad of dynamic barriers around Pleistocene Lake Carpentaria between Australia and New Guinea. During this phylogeographic survey, we discovered a large (134 Mbp) neo-Z chromosome and we explored its diversity, divergence and introgression landscape. We show that, as in some sylvioid passerine birds, a fusion occurred between chromosome 5 and the Z chromosome to form a neo-Z chromosome; and in *E. cyanotis*, the ancestral pseudoautosomal region (PAR) appears nonrecombinant between Z and W, along with most of the fused chromosome 5. The added recombination-suppressed portion of the neo-Z (~37.2 Mbp) displays reduced diversity and faster population genetic differentiation compared with the ancestral-Z. Yet, the new PAR (~17.4 Mbp) shows elevated diversity and reduced differentiation compared to autosomes, potentially resulting from introgression. In our case, long-read sequencing helped clarify the genomic landscape of population divergence on autosomes and sex chromosomes in a species where prior knowledge of genome structure was still incomplete.

KEYWORDS

Entomyzon cyanotis, genome assembly, introgression, long-read sequencing, neo-sex chromosome, phylogeography, population genomics

John T. Burley and Sophia C. M. Orzechowski share first authorship and contributed equally.

1 | INTRODUCTION

Revisiting classic phylogeographic study systems with genome-scale data can shed new light on the genomics and history of species (Cutter, 2013; Edwards et al., 2015; Nielsen et al., 2017; Peñalba et al., 2019; Stryjewski & Sorenson, 2017). Compared to multilocus phylogeography (e.g., Moritz et al., 2016) and the use of reduced-representation genome sequencing (e.g., Harvey & Brumfield, 2015), whole-genome phylogeography is most useful for discovery of structural variation and inference of natural selection on specific genomic regions (Brito & Edwards, 2009; Edwards et al., 2021). Whole-genome sequences provide an abundance of data and the ability to choose specific, putatively neutral loci for historical demographic analysis, although it is still unclear whether such data is superior for demographic inference compared to targeted locus data sets, such as ultraconserved elements (UCEs) or exon-capture. Long-read sequencing is currently expanding the domain of phylogeography beyond the monumental burst enabled over the last decade by affordable genome-wide, targeted-locus sequencing. For example, researchers have begun to use long-read sequencing across populations to explore the microevolutionary significance of structural genomic variants (Beyter et al., 2020; De Coster et al., 2021; Rech et al., 2022; Weissensteiner et al., 2020). A common strategy is to use long reads to characterize unknown chromosomal rearrangements in de novo genome assemblies and to combine these with short-read population sequencing to explore both the macroevolution of genomic rearrangements as well as their microevolutionary dynamics among populations. In this way, phylogeography in the era of long-read sequencing seems poised for even further integration of population genomics and genome evolution.

The biota of northern Australia and Papua New Guinea has long been recognized as a valuable system for studying speciation, with diverse taxa subject to vicariance in parallel across common biogeographic barriers (Bowman et al., 2010; Cracraft, 1986; Keast, 1961; Mayr, 1940; Schodde & Mason, 1999). In birds, deep phylogenetic splits within species and between sister species are observed across the Carpentarian Barrier (CB), a former large floodplain separating Cape York (CY) and forests of the east coast (EC) from a series of sandstone escarpments to the west constituting the "Top End" (TE) and Kimberley Plateau (KP; Jennings & Edwards, 2005; Lee & Edwards, 2008; Lamb et al., 2019; Peñalba et al., 2019; Toon et al., 2010). Divergence across the CB for savanna-adapted taxa is typically attributed to either the intrusion of the arid zone from central Australia to the Carpentarian coastline during Plio-Pleistocene glacial maxima, or to the intrusion of the Carpentarian Gulf waters inland towards central Australia (Bowman et al., 2010). Divergence times across the CB and other less prominent biogeographic barriers in the region (Figure 1; Bryant & Krosch, 2016; Cracraft, 1986; Edwards et al., 2017; Ford, 1978) are highly variable among taxa (Bowman et al., 2010; Edwards et al., 2016; Lee & Edwards, 2008); secondary contact occurs regularly, reflecting the dynamic nature of these barriers to gene flow (Lee & Edwards, 2008; Lopez et al., 2021; Toon et al., 2010).

Phylogeographic patterns in this region are complicated by the recurrent exposure and inundation of the continental shelf between Australia and Papua New Guinea (PNG) during the Pleistocene (Joseph, Bishop, et al., 2019). Two transient migration routes existed for savannah and mangrove adapted species: one between CY and PNG as recently as 7 ka with sea levels 15 m below present; and a second route between TE and PNG as recently as 12 ka with sea levels 55 m below present (Chivas et al., 2001; Kearns et al., 2011; Reeves et al., 2007, 2008; Figure 1; Supporting Information). When both land bridges were exposed, they were separated by a large inland lake, Lake Carpentaria, up to 250 km wide, 500 km long and 15 m deep on average (Jones & Torgersen, 1988; Reeves et al., 2008; Yokoyama et al., 2001). The effects of gene flow cessation across both migration routes is evident in conflicting phylogenetic patterns across taxa. A general species-area hypothesis, represented in Newick notation as ((KP, TE),((PNG,CY),EC)), originally proposed using cladistic methods (Cracraft, 1986), is often supported in phylogenetic studies (Bowman et al., 2010; Edwards, 1993a; Peñalba et al., 2019; Toon et al., 2017). However, certain taxa demonstrate closer genetic affinity between the TE and PNG than between CY and PNG – e.g. (((KP,TE), PNG), (CY,EC)) – despite the more recent and frequent connections between the latter throughout the past 2.5 million years (Dorrington et al., 2020; Pepper et al., 2017; Toon et al., 2017; Williams et al., 2008; Wüster et al., 2005). Mitonuclear phylogenetic discordance in butcherbirds has led authors to hypothesize introgression across the Arafura Shelf during Pleistocene glacial maxima for taxa with deep CB divergence (Joseph, Bishop, et al., 2019; Kearns et al., 2011, 2014).

Pleistocene sea level fluctuations, coupled with cyclic aridity in the CB resulted in a triad of distinct but transient gene flow barriers around Lake Carpentaria to the east, west and south (Figure 1). This probably provided opportunities for introgression, however, previous studies of Australo-Papuan taxa typically lack the genomic resolution or appropriate geographic sampling to test such hypotheses using formalized introgression statistics (but see Kearns et al., 2014). Secondary contact between PNG and TE for a species with a deepest divergence across the CB is predicted to leave a genomic signature of allele sharing between PNG and TE (potentially also KP) that is independent of CY, even if there is more recent shared genetic history between PNG and CY. Other scenarios of gene flow across non-sister populations were possible during Pleistocene species range fluctuations, and up to the present, in cases where reproductive incompatibility was never established during range contractions.

Using whole-genome data, we aimed to examine phylogeographic history and test the hypothesis of secondary contact across the Carpentarian barrier and Arafura Shelf for a system exhibiting a classic distribution across northern and eastern Australia. For this work we chose the blue-faced honeyeater (*Entomyzon cyanotis*), which we expect to have a phylogeographic history typical of codistributed taxa across this region (Figure 1). *E. cyanotis* is the only member of its genus and an ecological generalist, found across a range of habitats including mangroves, swamp forests and savannah – habitats likely to have been formed on

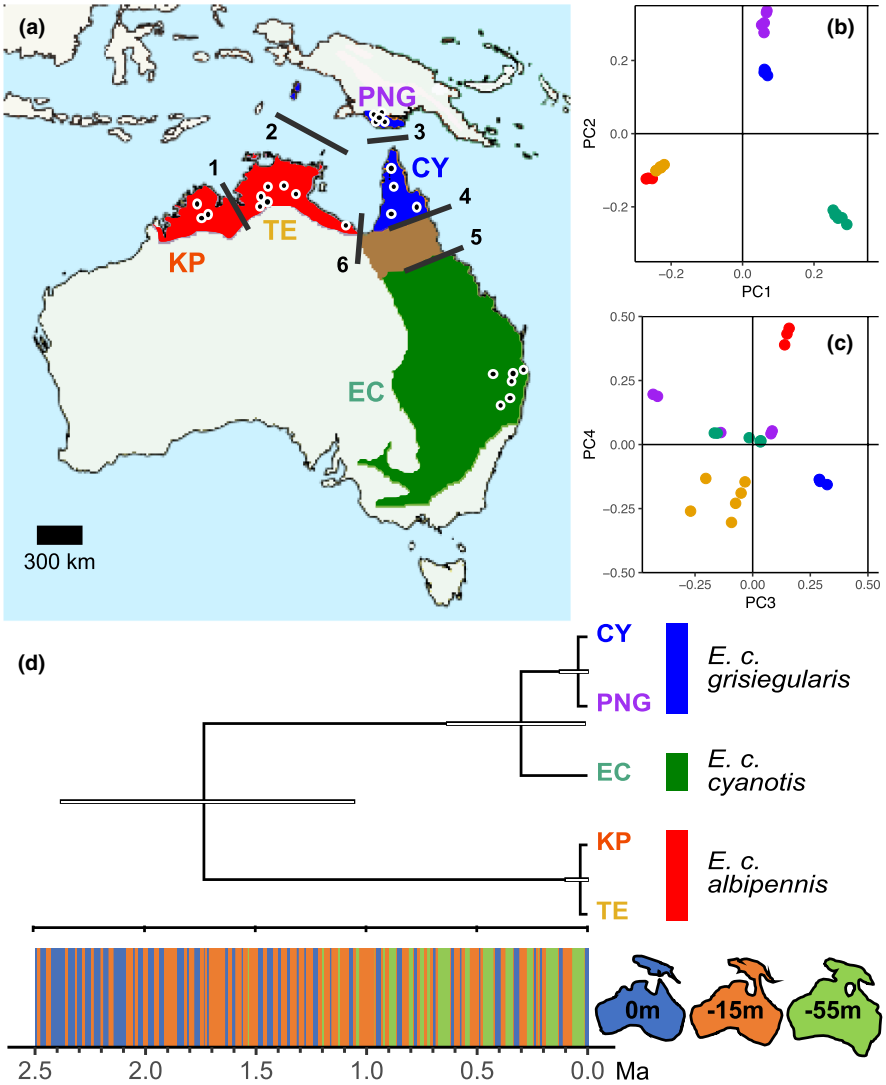

FIGURE 1 Geographic range, genetic structure and phylogeny of the blue-faced honeyeater. (a) the distribution of three *E. cyanotis* subspecies: *cyanotis* (green), *griseigularis* (blue) and *albipennis* (red). Brown shading indicates a hypothesized hybrid zone. Range map: Wikipedia commons, adapted from Shodde and Mason (1999). Black circles represent approximate sampling localities. Five populations identified in this analysis are depicted: East Coast (EC), Cape York (CY), Papua New Guinea (PNG), the Top End (TE), Kimberley plateau (KP). Common biogeographic barriers in this region are marked as black lines: Bonaparte gap (1), Arafura shelf (2), Torres Strait (3), Torresian gap (4), Burdekin gap (5), Carpentarian barrier (6). (b, c) PCA of autosome-wide SNPs for 24 individuals (points coloured by sampling locality), with the top four PCs explaining 16.1, 10.2, 4.5 and 4.4%, respectively. (d) Population divergence time estimates showing the 95% HPD (node bars) around the median obtained from 3,381 autosomal SNPs using SNAPP (Bryant et al., 2012). The time scale depicts temporal dynamics of three key landmass configurations of Australia and New Guinea at sea levels 0, 15 and 55 m below present levels, which putatively enabled range contiguity across the Torres Strait and Arafura shelf (Supplementary Text). Geological time scale is based on global sea level reconstructions by de Boer et al. (2014).

newly established land masses (Ford, 1982; Norman et al., 2007; Schodde & Mason, 1999). Three subspecies are recognized, based on phenotypic variation (Schodde & Mason, 1999) and supported by ddRAD data (Peñalba et al., 2019). The subspecies *E. c. albipennis* occurs west of the CB in tropical savannah, mixed eucalyptus forests and pandanus-dominated coastal habitats; *E. c. griseigularis* is found on the Trans-Fly Peninsula of PNG and CY; *E. c. cyanotis* occurs across most of the subtropical and temperate east coast of Australia (Schodde & Mason, 1999). A hybrid zone is thought to occur at the range intersection of *E. c. griseigularis* and *E. c. cyanotis*, based on observations suggesting interbreeding between these subspecies (Peñalba et al., 2017; Schodde & Mason, 1999).

In the course of our phylogeographic survey using a short-read de novo assembly, we discovered a neo-sex chromosome in *E. cyanotis* involving chromosome 5 (Chr5). This structural rearrangement involving the sex chromosomes adds to a growing list of avian neo-sex chromosome systems (Dierickx et al., 2020; Gan et al., 2019; Huang, Furo, et al., 2021; Leroy et al., 2019; Pala et al., 2012; Sigeman et al., 2020), in a clade previously noted for karyotypic stability (Ellegren, 2010). We then generated a second de novo assembly of

E. cyanotis using long-read nanopore sequencing data to characterize the neo-Z chromosome and determine its structural similarity to other recently characterized neo-sex chromosomes in passerines, and provide a foundation for examining its macroevolutionary and phylogeographic history. Sardell (2016) reported on a likely neo-sex chromosome in the genus *Myzomela* of the honeyeater family (Meliphagidae) using ddRAD data, but did not characterize the locus in detail. Our study thus presents the first well-characterized neo-sex chromosome in the honeyeater family.

The context of reticulate evolution in *E. cyanotis* combined with our nearly chromosome-level assembly of this previously uncharacterized major genomic rearrangement provides a new opportunity to explore the genomic landscape of diversity, divergence and introgression. Neo-sex chromosomes are potentially valuable for investigating the role of sex-linked genomic regions in speciation and adaptation (Bracewell et al., 2017; Kitano et al., 2009; Martin et al., 2020; Sardell, 2016). Yet, case studies are lacking from Z chromosomes containing portions in which recombination with the W has ceased very recently (Janes et al., 2009; Nam & Ellegren, 2008; Wright et al., 2014). Although theory predicts that the Z chromosome should carry lower genetic diversity and differentiate faster than autosomes as populations diverge due to increased drift and the possibility for linked selection (Bachtrog et al., 2011; Charlesworth et al., 1987; Pool & Nielsen, 2007), it is not clear from limited case studies (Mongue et al., 2021; Sigeman et al., 2021) whether or how population genetic patterns and processes on different strata of neo-Z chromosomes, including recently added portions, should vary. In addition, the existence of a new pseudoautosomal region (PAR) on the *E. cyanotis* neo-Z chromosome may provide a recombination hotspot, with potential consequences for introgression and adaptation (Janes et al., 2009; Otto et al., 2011). Thus, we further analysed our population resequencing data to see what additional phylogeographic insights could arise from population genomic analyses of the neo-Z chromosome.

2 | MATERIALS AND METHODS

2.1 | Fieldwork and specimens used

Fieldwork in eastern Australia producing samples now in the care of the University of Washington Burke Museum (UWBM) took place in 2002 and were loaned as part of this study. Fieldwork in Western Australia and New South Wales leading to samples now in the care of the Museum of Comparative Zoology (MCZ) took place in 2005 and 2019, respectively. Loans from the Australian National Wildlife Collection (ANWC) and University of Kansas Museum of Biodiversity (KU) provided additional samples from across the geographic range, including PNG. *Entomyzon cyanotis* samples were chosen to span the entire geographic range including five major areas of endemism as defined by Cracraft (1986; EC, CY, PNG, TE, and KP), aiming for 3–6 individuals (6–12 alleles/haplotypes) per region. We specifically avoided geographic regions where *E. cyanotis* subspecies were expected to undergo hybridization (Peñalba et al., 2017), erring towards a sampling scheme in which sampled individuals would likely represent their geographic population. Following best practices, all de novo genome assemblies and resequencing data generated in this study for the 26 individuals have associated museum specimen vouchers (Table S1, Buckner et al., 2021).

2.2 | De novo assemblies using short- and long-read sequencing

We first generated a de novo assembly from one male *E. cyanotis* (museum voucher accession number: MCZ Orn 336010) using short-read Illumina shotgun and mate-pair libraries and the ALLPATHS-LG assembly algorithm (Gnerre et al., 2011), following library preparation steps outlined in Grayson et al. (2017; Supporting Information). We aimed for a genome coverage of 55× by sequencing a short read library (220 bp) and a mate-pair library (3 kbp) across four sequencing lanes using Illumina HiSeq 2500. We hereafter refer to the resulting assembly as the "short-read assembly".

We later generated a second de novo assembly from one female *E. cyanotis* (museum voucher accession number ANWC B60257; museum tissue accession number MCZ Cryo 149706) using long reads obtained from Oxford Nanopore PromethION and MinION machines with the Flye (version 2.8.1-b1676) assembler (Kolmogorov et al., 2019), and polished with the long reads using Medaka (https://github.com/nanoporetech/medaka; Oxford Nanopore Technologies Ltd.; Supporting Information). Flye is a haploid assembler with a "nano-raw" option to account for the noisiness of raw nanopore reads as it collapses haplotypes. Medaka was designed to polish draft assemblies from Flye using a neural network approach on long reads in pileup format to identify and correct systematic errors. We did not polish the long-read assemblies with additional Illumina reads in part because we found that having high (>70×) nanopore read coverage and self-polishing with Medaka resulted in an assembly with BUSCO completeness scores similar to other high quality avian assemblies (Table S4; Peñalba et al., 2020). We note that artefacts and misassemblies such as frameshifts or homogenization of repetitive regions and paralogues can sometimes arise from excessive polishing (Peona et al., 2021; Rhie et al., 2021). Additionally, software tools like Medaka, Racon, and other long- and short-read-based polishing tools can sometimes fail to fix systematic errors, necessitating new polishing methods such as Homopolish, which instead leverage homologues from closely related lineages (Huang, Liu, et al., 2021). Best practices on polishing nanopore-based assemblies will likely continue to evolve alongside the continued improvement of nanopore sequencing accuracy. Our primary use of nanopore long-read assemblies was to inform the structure of the neo-Z chromosome, and to explore coarse-scale variation in population genetic parameters, which is unlikely to be adversely affected by additional polishing. Additional steps required to adequately assemble the neo-Z chromosome are described below and in Results. We hereafter refer to various iterations of this assembly as the "long-read assembly".

2.3 | Population resequencing, read mapping and variant calling using the short-read assembly

Whole genome-resequencing was performed on 24 *E. cyanotis* specimens across its geographic range, including the reference individual (Figure 1), as well as individuals from two species from the sister genus of *Entomyzon*, *Melithreptus albogularis* and *M. lunatus* (Supporting Information). We aimed for a per-individual read coverage of ~10× or slightly higher for a few of the individuals (Table S2), sequencing all individuals across four lanes of Illumina HiSeq 2500 with paired end 125 bp read length. Reads were filtered and trimmed for adapters using TrimGalore (https://github.com/FelixKrueger/TrimGalore), and quality was checked before and after trimming using FastQC to rule out systematic bias in quality between samples (http://www.bioinformatics.babraham.ac.uk/projects/fastqc/).

Reads of all individuals were mapped to the short-read assembly using BWA-MEM version 0.7.9 (Li & Durbin, 2009), after having first marked remaining adapter content in reads using Picard Tools version 1.119 (http://broadinstitute.github.io/picard/). Duplicate read removal was performed using Picard Tools, and indel realignment was performed using GATK version 3.7.0 (McKenna et al., 2010). Variant calling was performed using GATK joint genotyping of either (a) 24 *E. cyanotis* samples (for population analyses), or (b) 24 *E. cyanotis* samples plus 2 *Melithreptus* samples for analyses requiring an outgroup. On this SNP set, filtering was performed following the GATK recommendations and checking distributions of the following metrics: QD > 2.00 (quality by depth), DP < 700 (per-base depth of coverage, for all samples), −0.5 < BaseQRankSum < 0.5 (base quality), SOR < 3.0 (strand odds ratio, for detecting strand bias, −4.0 < ReadPosRankSum < 4.0 (rank sum test of base calls relative to proximity to read edge).

2.4 | Classification of Z-linked scaffolds in the short-read assembly

Male samples (homogametic - ZZ) were preferentially chosen for sequencing over females which are heterogametic (ZW), as is typical in population genomic studies of birds. However, a total of seven female specimens from three populations (TE, PNG, EC) were included in the dataset due to limited availability of male samples as well as sex misidentification of three specimens, which we confirmed post hoc using sexing PCR (Fridolfsson & Ellegren, 1999). To initially confine our population studies to autosomal scaffolds, scaffolds belonging to the Z-chromosome of *E. cyanotis* were identified by calculating the per-scaffold coverage ratio of males to females using seven samples of each sex. Scaffolds were initially designated as linked to the Z-chromosome if the per-scaffold coverage ratio of males to females was close to 2, and if the difference in read count between sexes was statistically significant ($p < .05$, following Lamichhaney et al., 2016). This method effectively removed all scaffolds with major synteny to the zebra finch (*Taeniopygia guttata*) Z chromosome, but did not remove all sex-linked scaffolds due to the presence of relatively young neo-sex chromosomes, as we discovered during subsequent analyses (see Results and Figures S7–S9).

2.5 | Population genomic analyses based on the short-read assembly

We used ANGSD, ngsTools and related programs for subsequent population genetic analyses using genome-wide SNPs mapped to the short-read assembly (Fumagalli et al., 2013, 2014; Korneliussen et al., 2014). We performed PCA on a covariance matrix of genotype similarities among the 24 *E. cyanotis* samples based on ~6 million SNPs from all autosomal scaffolds >100 kbp. Using ANGSD, heterozygosity per base pair (i.e., genetic diversity, π) and Tajima's *D* were calculated for each population as was genetic differentiation (F_{ST}) between populations and between subspecies. Only the male samples were used when performing these analyses on the neo-Z chromosome. We performed the ABBA-BABA test for site heterogeneity between four taxa (Durand et al., 2011) for each of the 10 possible arrangements of three taxa plus an outgroup that maintained the overall topology supported by our data. These tests produce the statistic "Patterson's *D*", which was used to assess evidence for gene flow between nonsister lineages in a trio of *E. cyanotis* populations. We used our *M. albogularis* sample to designate the ancestral allele in all topology tests (ANGSD chose an allele at random from the outgroup if it was heterozygous at a relevant site) and selected one male sample with genome-wide coverage close to 9× to represent each population, to minimize any possible bias resulting from coverage differences. Jackknife standard errors of Patterson's *D* were calculated using a block size of 100 kbp. *Z*-scores were used to assess the statistical significance of gene tree heterogeneity, taking an absolute value above 3 as an indication of statistical significance (as in Patterson et al., 2012; Supporting Information). For all calculations except for estimation of windowed π, we used the -sites flag in ANGSD to restrict analyses to only the SNPs passing GATK filtering. The different treatment for π estimates was implemented so that ANGSD used the appropriate number of callable bases per window as the denominator.

We used TreeMix (Pickrell & Pritchard, 2012) to infer population splits and mixtures based on allele frequencies of autosome-wide SNPs calculated for all populations and for both *Melithreptus* samples, and which passed filtering following the GATK best practices. Finally, we used the program EEMS (Petkova et al., 2016) to produce interpolated surfaces of spatial genetic variation and effective migration rates using a heavily filtered set of ~68,000 autosome-wide SNPs. We filtered the SNPs for this analysis in order to find a SNP set that fulfilled the assumptions of the EEMS distance matrix and also because full genome-wide SNPs are not necessary for this particular analysis.

2.6 | Estimates of divergence time

Divergence times were estimated with SNAPP (Bryant et al., 2012) using a strict clock model and linked population sizes, following Stange

et al. (2018) and Fang et al. (2020). To reduce run time, this analysis was performed using 3381 SNPs across all autosomes filtered to require genotype calls for 90% of individuals per site and to exclude SNPs closer than 1 kbp. Additionally, a constraint tree was used to prevent the MCMC from exploring topologies other than that supported by clustering of the population genetic dissimilarity matrix from the full autosomal SNP set using the neighbour-joining method (Saitou & Nei, 1987) implemented in the R package, APE (Paradis et al., 2004; Supporting Information). A prior of 1.8 Ma with a standard deviation of 0.2 was placed on the divergence time across the Carpentarian Barrier, following the only available previous estimate for *Entomyzon* across this same barrier based on mtDNA (Toon et al., 2010). A generation time of 2 years was assumed based on reports of ~1.5 year maturation time of adult facial coloration and breeding over several years (Higgins et al., 2020). We acknowledge that generation time is critical for estimating divergence times accurately and that more precise estimates of generation time, ideally based on demographic data, are needed for such analyses (Bakker et al., 2022; Jonasson et al., 2022).

2.7 | Population genomic analyses of the neo-Z chromosome using the long-read assembly

We mapped filtered reads from all male samples ($n = 17$) to a subset of scaffolds in the long-read assembly representing the neo-Z chromosome and Chr1A. Chr1A was chosen to represent autosomes because it is similar in length to the ancestral Chr5 as well as the ancestral-Z chromosome, and it is acrocentric (in zebra finch) like Chr5 (Dos Santos et al., 2017). Read mapping, duplicate removal and indel realignment were performed as described above for genome-wide sequencing data mapped to the short-read assembly. In this case, however, variant calling was performed using Samtools mpileup (Li et al., 2009). A different set of bioinformatic tools was used for SNP calling and analysis using the long- and short-read assemblies because pixy, unlike ANGSD, provides a formalized approach to calculate d_{XY} and because Samtools was a faster way to obtain the input files for pixy and Dsuite than GATK. We used pixy (Korunes & Samuk, 2021) to estimate genetic diversity within and between populations (π and d_{XY}, respectively) in nonoverlapping 50 kbp windows on specific regions of the neo-Z chromosome (see Results) and Chr1A. The Dsuite program (Malinsky et al., 2021) was used to calculate introgression statistics separately for those genomic regions in 3000-SNP windows, rather than fixed-size windows, to avoid bias in the power to detect introgression caused by sample size variation. In contrast to the analysis implemented in ANGSD, Dsuite utilizes all samples in a population rather than a single individual per population. The modified *f* statistic, f_{dM}, is reported in these tests because it has less variance than Patterson's *D* in small genomic windows; positive and negative values reflect introgression between P3–P2 and P3–P1, respectively, for a trio of populations defined as ((P1,P2),P3) (Malinsky et al., 2015, 2021; Martin et al., 2015). For significant f_4-ratio tests ($p < .01$) in Dsuite, *f*-branch statistics were used to assign introgression evidence from *f* statistics to internal or external branches of the population phylogeny. In this analysis, *M. albogularis* and *M. lunatus* were used as outgroups. All data sets have been deposited in relevant databases, including ancillary data deposited in Dryad [data set] (Edwards et al., 2022).

3 | RESULTS

3.1 | *Entomyzon cyanotis* genome assemblies

The short-read assembly used a total of 79.5 GB of raw data, including ~360 million reads from the fragment library and ~450 million reads from the mate-pair library. We obtained 64.5× coverage and produced an assembly totaling 1.03 Gbp, representing 93.6% of the estimated genome length of 1.1 Gbp, and with a contig and scaffold N50 of 168 kbp and 4.6 Mbp, respectively, which places it in the top 31% of short-read avian assemblies reviewed in Bravo et al. (2021) as of January 2021. This assembly contains 94.5% complete benchmarking orthologues in the BUSCO avian set aves_odb9 (Simão et al., 2015; Table S4), and contains 507 scaffolds larger than 100 kbp (of 3504 total), which we have analysed in population genomic analyses presented here unless otherwise stated. We generated the long-read assembly from 7.1 million long reads (mean coverage 72×) sequenced on PromethION and MinION with a combined read length N50 of 16,771 bp (Table S3). The prepolished long-read assembly had a fragment (assembled contigs and scaffolds) N50 of 28.9 Mbp and total length of 1.082 Gbp, and contains 90.1% of benchmarking orthologues (present and complete) from the BUSCO aves_odb9 database (Table S4; Simão et al., 2015).

3.2 | Population structure and phylogenetic inference

The per-sample sequencing depth among the 24 resequenced *Entomyzon* individuals ranged from 7.33 to 38.85 (mean = 11.22), calculated as the total number of bases with Q ≥ 30, divided by the estimated genome length for *E. cyanotis* (1.1 Gb). A principal component analysis (PCA) based on approximately 6 million autosomal SNPs shows that geography is a major factor influencing genetic differentiation in *E. cyanotis* (Figure 1). The first two principal components (PCs, total variance explained = 26.3%) together separate samples into three main clusters corresponding to *E. cyanotis* subspecies based on morphological variation (Schodde & Mason, 1999), mitochondrial (ND2) data (Toon et al., 2010) and RAD sequencing data (Peñalba et al., 2019). Clustering of samples within subspecies was also evident in the first two PCs, but more prominently in the third and fourth PCs (total variance explained = 8.9%). Five populations identified by PCA are monophyletic, based on a neighbour-joining tree obtained with autosome-wide SNPs (Figure S4).

Using SNAPP and priors on divergence time from previous work, we estimated that *E. cyanotis* diverged across the Carpentarian Barrier approximately 1.70 Ma (95% highest posterior density [HDP]:

1.04–2.38 Ma), based on a coalescent model that assumes no gene flow after divergence, fixed population size and a generation time of 2 years (Figure 1d). The mean estimate of CB divergence time was reduced to 1.5 Ma when the standard deviation of the prior was increased from 0.2 to 0.4; however, the following estimates were more robust to this change. We estimated divergence between the subspecies *griseigularis* in CY-PNG and *cyanotis* in EC at approximately 0.27 Ma (95% HDP: 0.01–0.64 Ma; Figure 1d). Based on present-day distributions, these subspecies likely diverged across a barrier in the region of the Torresian and Burdekin Gap (Figure 1), although our sampling does not allow us to rule out divergence across the Torres Strait followed by subsequent migration into CY before a second split across the Torres Strait. Divergence times within subspecies *grisiegularis*, between CY and PNG, likely occurred in the past 123 ka based on the 95% HPD (Figure 1d). This divergence is consistent with reduced gene flow caused by the inundation of Torres Strait, which most recently occurred approximately 7, and 130 ka before that (Figures 1d and S3). Divergence time within subspecies *albipennis*, between KP and TE, is spatially consistent with hypothesized barriers in the region of the Bonaparte Gap and occurred in the past 98 ka based on the 95% HPD (Figure 1d).

3.3 | Population genetic diversity and differentiation

Autosome-wide genetic diversity (π) varies from 0.0019 (EC) to 0.0031 (TE and CY; Figure 2a; Table S7). The EC population has substantially lower π than other populations, with median π close to or less than the lower quartile of other populations (Figure 2a; Table S7), which may reflect a historical EC population size reduction. Tajima's *D* is positive in most 50 kbp windows of autosomes for KP, PNG and EC, while the median Tajima's *D* is marginally below zero for TE and CY (Figure 2b; Table S7).

Pairwise genetic differentiation (F_{ST}) between the subspecies is expected to mirror relative divergence times in the absence of genome-wide effects of introgression, selection or population size fluctuations. This expectation is met on the Z chromosome but not on autosomes (Figure 2c). On the Z chromosome (see below for characterization of the ancestral- and added- portions), differentiation is, as expected, lowest between the most recently diverged subspecies pair *griseigularis–cyanotis* (ancestral-Z median $F_{ST} = 0.237$). Whereas, on autosomes, differentiation between recently diverged *griseigularis–cyanotis* (median $F_{ST} = 0.159$) is slightly higher than between *albipennis–griseigularis* (median $F_{ST} = 0.152$; Figure 2c). This discrepancy may be caused by autosome-biased introgression between *albipennis* and *griseigularis* that would reduce differentiation between them relative to the *albipennis–cyanotis* comparison (median $F_{ST} = 0.244$; Figure 2c).

In general, spatial patterns in genetic diversity and differentiation are recapitulated in estimated effective migration and diversity surfaces generated using EEMS (Petkova et al., 2016). A broad region of low effective migration – where genetic similarity declines more rapidly per unit area than the range-wide average rate – covers the CB and eastward to the broadly defined Torresian Gap, dividing the three recognized *E. cyanotis* subspecies (Figures 2d and S5). The effective diversity surface generally recapitulates higher diversity towards the geographic centre of the *E. cyanotis* range, albeit divided by the Gulf of Carpentaria (Figures 2e and S5). The EEMS analysis also demonstrated that the genetic structure in *E. cyanotis* is unlikely due to isolation by distance.

3.4 | Tests of introgression on genome-wide SNPs

We ran ABBA-BABA tests for each of the 10 possible 4-taxon topologies possible with five *E. cyanotis* populations, given the phylogeny inferred from genome-wide SNPs, with *M. albogularis* used to designate the ancestral allele in all cases. From across the autosomes, tests used ~844,000 (±50 K) biallelic SNPs per topology test (Table S5). An excess of ABBA sites in the topology test (((PNG,CY),EC),O) indicates the occurrence of gene flow between CY and EC, independently of PNG ($D = 0.07$; $Z = 23.3$; Figure 3a). Similarly, an excess of ABBA sites in the topology test (((EC,CY),TE),O) indicates the occurrence of gene flow between CY and TE, independently of EC ($D = 0.10$; $Z = 38.1$; Figure 3a). Given that a similar result to the previous test – (((EC,CY),TE),O) – is obtained by replacing CY with PNG and/or replacing TE with KP (Table S5), these four tests together indicate that gene flow occurred between *E. c. griseigularis* and *E. c. albipennis* since the former diverged from *cyanotis* and prior to splits within *griseigularis* and *albipennis* (Figure 3a). However, in the topology test (((PNG,CY),TE),O), a small but statistically significant excess of BABA sites indicates that gene flow also occurred between PNG and TE independently of CY ($D = -0.01$; $Z = -3.13$; Figure 3a; Table S5). The TreeMix model with two migration edges provided the greatest reduction in the residual error matrix, supporting gene flow from an ancestor of the EC population into CY and from the common ancestor of CY and PNG to the common ancestor of TE and KP (Figures 3b and S6).

3.5 | Evidence for an autosome-Z fusion from male/female resequencing

During preliminary analyses of population genetic structure described above, we discovered 10 scaffolds summing to 37.2 Mbp in the short-read assembly (of the scaffolds >100 kbp) that starkly conflicted with the genome-wide pattern of population genetic structure, most readily observed in PCAs restricted to those scaffolds (Figure S7). We performed sexing PCR on all samples and found that sex was the driving factor of genetic structure on these scaffolds (Figure S7; Supporting Information). These scaffolds were not characterized as sex-linked in our protocol for identifying Z-linked scaffolds due to equal read depth from male and female samples, yet they showed higher SNP density for females in a VCF generated assuming diploidy in variant calls (Figure 4; Supporting Information).

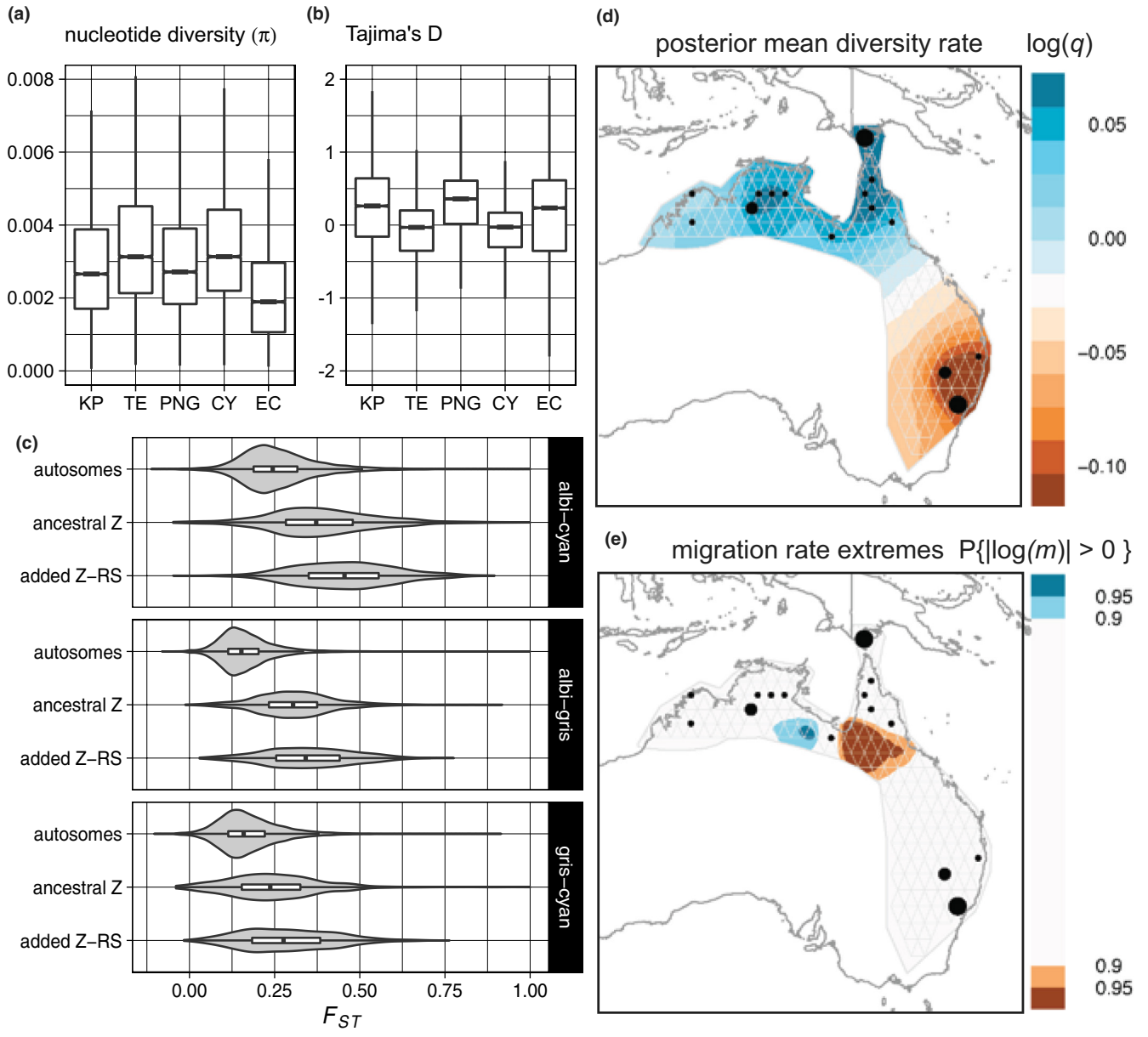

FIGURE 2 Spatial patterns in genetic diversity, differentiation and migration. (a, b) the distribution of nucleotide diversity per base pair (π) and Tajima's *D* for *E. cyanotis* populations across all autosomes in 50 kbp windows. (c) the distribution of weighted F_{ST} between *E. cyanotis* subspecies in 50 kbp windows, comparing the autosomes, ancestral-Z chromosome, and the recombination-suppressed (RS) portion of the added-Z. (d) Interpolated surface of genetic diversity (*q*) on the $\log_{10}$ scale. (e) regions where the interpolated migration rate (*m*) is significantly different to the mean. Boxplots depict the median (centre bar), 95% confidence intervals (notches) in (a, b), interquartile range (IQR; box extents) and the extent of values <1.5*IQR beyond box edges (whiskers), with the outliers removed for clarity. Plots d and e were generated using the package EEMS (Petkova et al., 2016).

In addition, alignments between the short-read assembly and zebra finch genome (tgut3.2.4) showed that the 10 sex segregating scaffolds are homologous to zebra finch Chr5 (Figure 4). We found evidence of physical linkage between Chr5 and a small portion of Z on scaffold 31 of the short-read assembly as well as a transition between autosomal and sex-linked sequence on scaffold 161 (Figures S8 and S9). These patterns suggested a neo-Z fusion and a physically linked PAR region, although with only these data at the time, we could not rule out misassembly errors. We therefore generated an independent long-read assembly to verify this possibility.

3.6 | Further resolution of the neo-Z from long-read sequencing

The initial long-read assembly of a female was highly contiguous (ONT-Flye, contig N50 = 28.9 Mbp, Table S4), with the stark exception of a highly fragmented (387 contigs, 1 scaffold) 37.2 Mbp region homologous to zebra finch Chr5 (Figures 5 and S1). The version of this long assembly that was polished with Medaka and used in subsequent analyses is ONT-Flye-Medaka-v1 (Table S4). We defined the portion of Chr5 that putatively fused to the Z in

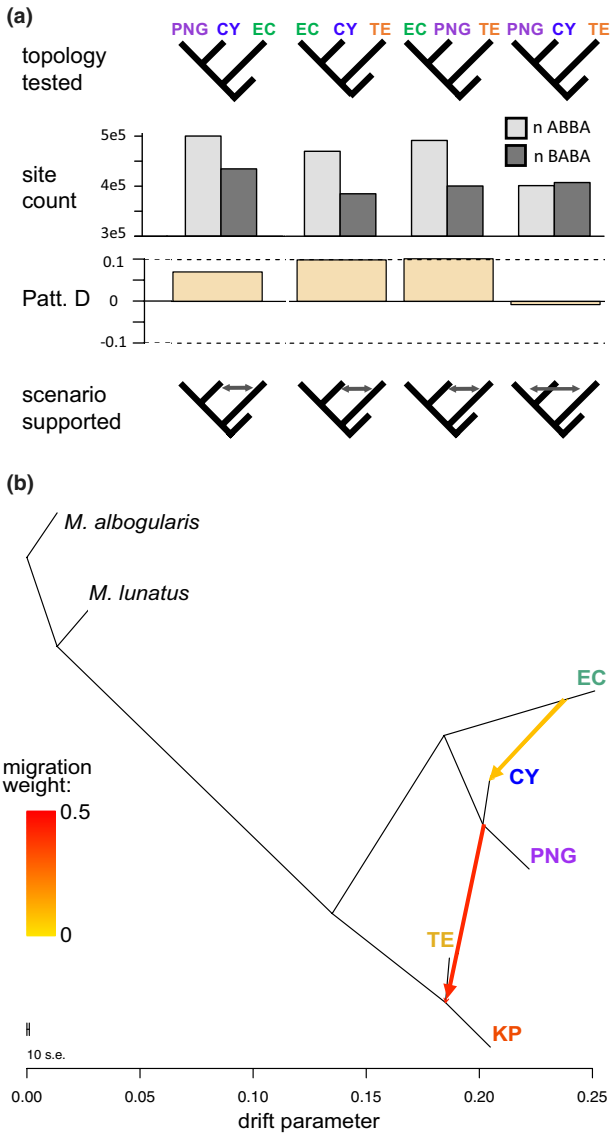

FIGURE 3 Inference of recent and ancient admixture. (a) ABBA-BABA results showing evidence for asymmetric gene flow in four topology tests (remaining six topology tests shown in Table S5). Patterson's *D* is statistically significant in all cases ($|Z| > 3$). (b) TreeMix graph with two migration edges coloured by migration weight.

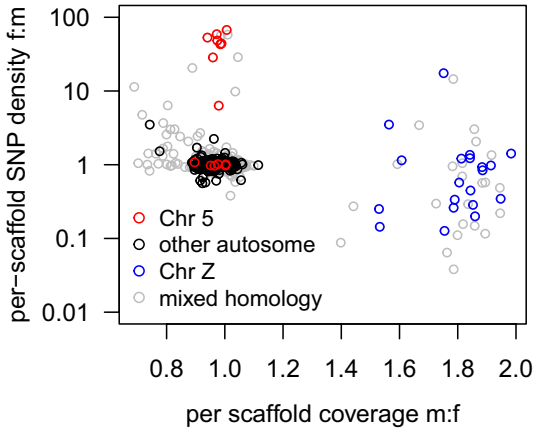

FIGURE 4 Evidence for a neo-Z chromosome from the short-read assembly and population resequencing. The scatterplot shows the per-scaffold SNP density sex ratio plotted against the read coverage sex ratio for scaffolds >100 kbp ($n = 507$). High SNP density f:m in some scaffolds syntenic to zebra finch Chr5 occurs because reads from both added-W and added-Z mapped to the male reference genome (demonstrated by equal m:f coverage), leading the genotyping algorithm to call heterozygous sites wherever the added-W and added-Z differ. Note that the ancestral W chromosome is highly degenerated so that those reads tend not to map to Z-linked scaffolds. Colours represent scaffold homology to zebra finch (Tgut 3.2.4) Chr5 (red), other autosomes (black) and Z chromosome (blue). Grey points represent *E. cyanotis* scaffolds that share homology to more than one scaffold of Tgut 3.2.4, even if belonging to the same chromosome.

E. cyanotis as the "added Z", following the terminology of Sigeman et al. (2021). The other haplotype would then be called the "added W" because it can no longer segregate randomly with respect to sex and, regardless of its fusion status, must be inherited with the ancestral W to avoid major genomic imbalances (Beukeboom & Perrin, 2014). We speculated that this 37.2 Mbp region of Chr5 was likely fragmented due to the level of divergence between the added-W and added-Z – lower than between ancestral sex chromosomes but higher than between typical autosome pairs (Figure S2) – which would lead to fragmentation as the haploid assembly algorithm attempted collapse the haplotypes (Guiglielmoni et al., 2021). The total length of the 388 fragments syntenic to Zebra Finch Chr5 was 70.3 Mbp, only ~8.7 Mbp larger than the length of zebra finch Chr5 (61.6 Mbp), indicating that the recombination-suppressed (RS) region of the added-Z/W (37.2 Mbp) was mostly not assembling into separate haplotypes, unlike the highly diverged ancestral-Z and W. We inferred that recombination between added-Z and -W had been suppressed in this 37.2 Mbp region from the highly elevated SNP density in females compared to males. Henceforth we will refer to this region of the neo-Z as "added-Z-RS".

To improve the fragmented, collapsed, and likely chimeric assembly of the added-Z, we therefore isolated PromethION reads from this region and mapped them to the homogametic (male) short-read assembly using Minimap2 (Li, 2018), focusing first on the scaffolds determined to be sex-linked and syntenic to zebra finch Chr5 (see Figures 4 and S8). Using BLAST-like percent identity (Figure S2) and the recombining PAR of the added-Z/W as a control, we were able to isolate reads specific to the added-Z, and, after two rounds of assembly, mapping, and polishing, generated two refined assemblies of the added-Z. We termed these versions of the long-read assembly using an abbreviation for Oxford Nanopore Technology (ONT): ONT-addedZ-v1 and ONT-addedZ-v2 (Figure 5). The final assembly of the added-Z (ONT-addedZ-v2) was 62.18 Mbp and consisted of 4 fragments, the largest (contig 4) being 55 Mbp, which we focus on here (Figure 5; Supporting Information).

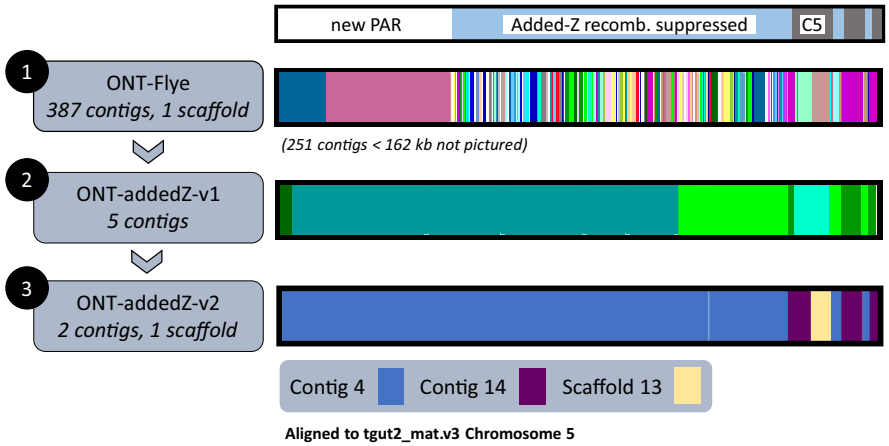

FIGURE 5 Refinement of the long-read added-Z assembly. The region of the added-Z which no longer recombines with the added-W (added-ZRS) was highly fragmented in the initial long-read assembly, which contained a total of 387 contigs and 1 scaffold homologous to zebra finch Chr5, summing to 70.34 Mbp. Of these, 251 contigs (summing to 11.3 Mbp) were not visualized with Satsuma and likely included added-W or chimeric added-Z/W haplotypes (Figures S1 and S2). After filtering and assembling added-Z reads (see Results and supporting information), the ONT-addedZ-v1 assembly contained 5 contigs. ONT-addedZ-v2 (assembled from filtered reads mapping to ONT-addedZ-v1) contained 2 contigs and 1 scaffold (one contig <6 kp was removed). 'C5' denotes unplaced autosomally-behaving fragments that are not physically connected to the new PAR in ONT-addedZ-v2 (contig 14 and scaffold 13).

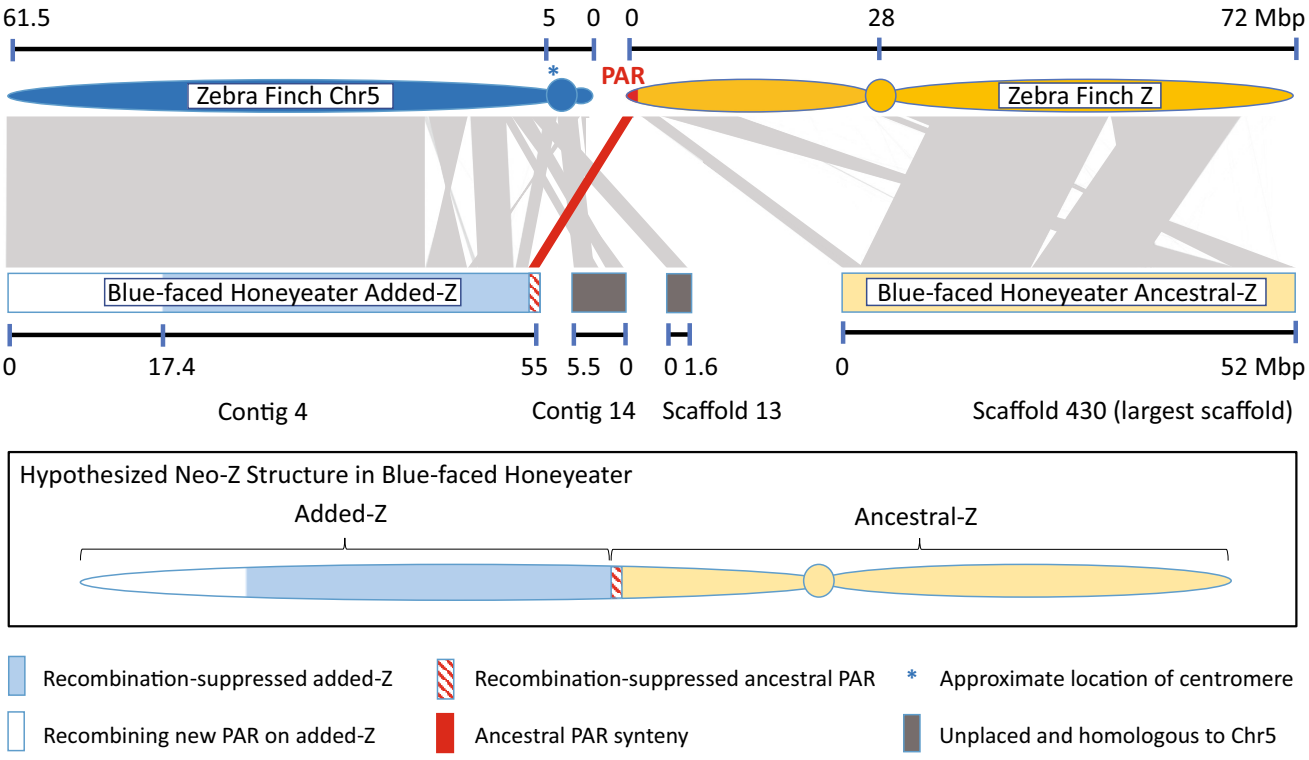

FIGURE 6 Evidence for the physical structure of the *E. cyanotis* neo-Z chromosome based on synteny to zebra finch (bTaeGut2.Mat.v3). The largest of three contigs in ONT-addedZ-v2 (contig 4) is almost entirely syntenic with zebra finch Chr5 (q-arm) with the exception of 380 kbp that is syntenic with zebra finch Z-PAR. Around this putative point of Z-autosome fusion, ancestral PAR is nonrecombinant between Z and W in *E. cyanotis*, along with 37.2 Mbp of the added-Z, while 17.4 Mbp of contig 4 displays characteristics of a "new" PAR. We cannot ascertain whether a drastically truncated Chr5 exists in *E. cyanotis*, comprised of scaffold 13 and contig 14 that are approximately syntenic to the p-arm and centromeric region of zebra finch Chr5, or whether these regions are physically linked to the neo-Z but failed to assemble with the larger contig. Synteny visualized with FastANI (Jain et al., 2018). Centromere locations derived from Knief and Forstmeier (2016).

3.7 | Resolving the structure and fusion of the neo-Z with synteny mapping and multispecies alignments

Using Satsuma (Grabherr et al., 2010), we performed synteny mapping between the short- and long-read assemblies and determined that the first 17.1 Mbp of contig 4 from ONT-addedZ-v2 constitutes part or all of the new PAR (Figure S10). The rest of contig 4 is syntenic to the 10 sex-linked scaffolds identified in the short-read assembly (Figures S8 and S10). Synteny mapping the long-read added-Z assembly (ONT-addedZ-v2) to zebra finch (bTaeGut2.mat.v3) indicated that the majority of contig 4 is homologous to the q-arm of the acrocentric Chr5 in zebra finch (Figure 6), where the centromere is designated as near the beginning of the chromosome (Dos Santos et al., 2017; Knief & Forstmeier, 2016). At the end of contig 4 (at 54.6 Mbp), a 380 kbp region is syntenic to the beginning of the Z chromosome in zebra finch, which is the location of the ancestral PAR (Ponnikas et al., 2022; Figure 6).

We then performed a multispecies pairwise alignment using AliTV (Ankenbrand et al., 2017), focusing on the putative fusion point between *Entomyzon* Chr5 and the ancestral-Z-PAR (Figures 7 and S11). We aligned this region in seven species, including the zebra finch and collared flycatcher, for which the PAR scaffolds were known a priori (Ponnikas et al., 2022; Smeds et al., 2014). This analysis again suggested that the end of contig 4 contains a putative fusion point between Chr5 and ancestral-Z on the PAR end (Figure 7). In all assemblies except zebra finch (which is chromosome-level), the PAR scaffolds were small and unplaced, suggesting that this region is generally hard to assemble in most species and may help explain why we could not assemble a longer pseudomolecule of the entire neo-Z even with long reads. This analysis also suggested that the *Entomyzon* neo-sex chromosome system is absent in the superb fairywren (*Malurus cyaneus*; Peñalba et al., 2020), which is estimated to have diverged from *Entomyzon* 30 Ma (Oliveros et al., 2019). We also unexpectedly found that the previously described neo-sex chromosome fusion involving Chr5 and Z-PAR in the horned lark (*Eremophila alpestris*) and Eurasian skylark (*Alauda arvensis*; Dierickx et al., 2020; Sigeman et al., 2019; Sigeman, 2021) involved the same region on the translocated *Entomyzon* Chr5, despite these being independent translocation events (Figure 7).

3.8 | Diversity, differentiation and evidence for introgression across the neo-Z chromosome

Using our long-read assembly, we characterized variation in genetic diversity, differentiation and evidence for introgression along two contigs representing the near-complete neo-Z chromosome, and

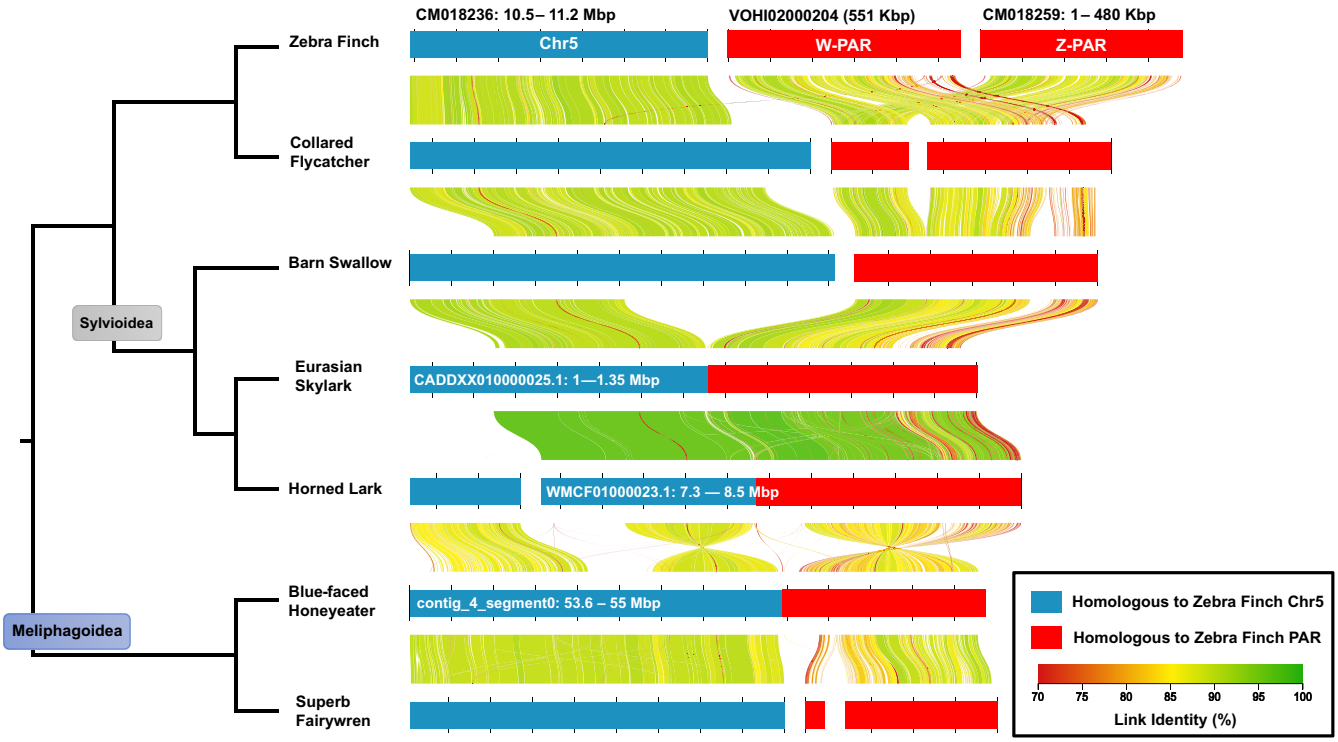

FIGURE 7 Convergent translocations involving Chr5 and the Z-PAR in *E. cyanotis* and larks (Alaudidae in Sylvioidea sensu Sigeman, 2021). Pairwise alignments of 7 songbird genome assemblies focusing on the end of contig 4 (53.6–55 Mbp) where the putative point of fusion between Chr5 and Z-PAR occurs in ONT-addedZ-v2. Neo-sex chromosomes have been described in Sylvioidea where all species carry a translocation between Chr4A and Z/W, which additionally involves Chr5 and Chr3 in most or all lark species (Sigeman et al., 2019). We discovered that the Chr5-Z-PAR fusion point in the male horned lark assembly (CLO_EAlp_1.0) and in the male Eurasian skylark assembly (GCA_902810485.1_skylark_genome) occurs in the same place as *E. cyanotis*, indicative of a convergent fusion between Chr5 and Z-PAR. The alignment was created with AliTV (Ankenbrand et al., 2017).

three contigs representing Chr1A as a control (Figure 8). Mean π across populations in 50 kbp windows varies significantly between the new PAR and the added-Z-RS, the ancestral-Z-PAR, the ancestral-Z and Chr1A (one-way ANOVA; $F_{4,3517} = 179.3$; $p < .001$; Figure 8a). Post hoc tests showed that means of π from all regions differ except that the ancestral-Z-PAR is not different to either the added-Z-RS or the ancestral-Z (Tukey's post hoc $p < .05$ for all other comparisons; Figure 8a), suggesting that the ancestral-Z-PAR is affected by recombination suppression just as in physically close portions of the added- and ancestral-Z. We therefore considered the ancestral-Z-PAR as linked to the RS region of the neo-Z chromosome in subsequent comparisons. The new PAR (mean $\pi = 0.0043$) displays slightly higher π than autosomes (Chr1A mean $\pi = 0.0037$, *pixy* estimate; autosome-wide mean $\pi = 0.0031$, *ANGSD* estimate) despite being physically linked to the RS portion of the added-Z, which has even lower π (mean = 0.0016) than the ancestral portion of the neo-Z chromosome (mean $\pi = 0.0022$; Figure 8a; Table S8), resulting in a substantial transition in π along the neo-Z, particularly on the added portion (Figure 8e).

For the most genetically distant population pair (KP-EC), F_{ST} in the neo-Z chromosome varies significantly between the new PAR, added-Z-RS and ancestral-Z (Tukey's post hoc $p < .005$; Figure 8b). For KP-EC, F_{ST} is lowest on the new PAR (mean = 0.39), followed by Chr1A (mean = 0.44), then the ancestral-Z (mean = 0.58), and is highest on the added-Z-RS (mean = 0.64; Figure 8b). This pattern of F_{ST} variation between regions is not observed for the least divergent pair (KP-TE), for which F_{ST} is significantly higher on Chr1A (mean = 0.10) than all other regions (Tukey's post hoc $p < .00001$), while F_{ST} for the new PAR is not different from that for the sex-linked regions (Tukey's post hoc $p > .3$; Figure 8b).

Evidence for recent introgression between CY and EC independently of PNG, which was supported in autosome-wide ABBA-BABA tests (Figure 3; Table S5), varies significantly among genomic regions tested here (one-way ANOVA; $F_{3,272} = 9.9$; $p < .00001$; Figure 8d). Here, we report the modified f_4-ratio statistic f_{dM} calculated in 3000-SNP windows, which can be interpreted as relative amounts of gene flow between P3–P2 (positive values) or P3–P1 (negative values), again for a trio of populations defined as ((P1,P2),P3); see Methods and Malinsky et al. (2021). The new PAR appears to be strongly affected by this recent gene flow between CY and EC, with 83.7% of windows ($n = 43$ windows) having $f_{dM\ ((PNG,CY),EC)} > 0$ (mean $f_{dM\ ((PNG,CY),EC)} = 0.024$, IQR = 0.010–0.039; Figure 8c,h). Evidence for introgression is also evident across Chr1A, albeit with lower mean and more variability across windows (mean $f_{dM\ ((PNG,CY),EC)} = 0.015$, IQR = −0.005–0.035, $n = 145$ windows; Figure 8c,h). By contrast, added-Z-RS does not show a strong or consistent signal of this recent introgression (Figure 8c). Evidence for introgression in the topology test ((EC,CY),TE) – a test supporting ancient gene flow between *albipennis* and *griseigularis* since the latter split from *cyanotis* but prior to splits within the subspecies (Figure 3; Table S5) – is generally positive across all regions tested here irrespective of sex-linkage (74.6% of windows having $f_{dM\ ((EC,CY),TE)} > 0$, mean = 0.024, $n = 307$; Figure 8d,i), with no significant difference between $f_{dM\ ((EC,CY),TE)}$ on the new PAR and other regions (Tukey's post hoc $p > .5$), although lower than on Chr1A (Tukey's post hoc $p = .03$; Figure 8d,i).

We calculated *f*-branch statistics to assign evidence of gene flow to specific branches using correlated f_4-ratio tests (Malinsky et al., 2018, 2021). This analysis demonstrates that autosomally-recombining sequence (new PAR and Chr1A) show greater evidence for introgression than sex-linked sequence (added-Z-RS and ancestral-Z; Figure 9). We also note that the directional introgression from CY to EC supported by *f*-branch statistics is in a direction opposite to the migration edge inferred in the TreeMix analysis (Figure 3b). Finally, *f*-branch statistics provide additional support for the hypothesis of gene flow between PNG and the TE and KP independently of CY, which would most probably have occurred when the Arafura Shelf was fully exposed during Pleistocene glacial maxima (Figures 1d and 9).

4 | DISCUSSION

4.1 | Phylogeography of *Entomyzon cyanotis*

The key finding from our whole-genome phylogeographic analysis is that the genetic history of *E. cyanotis* is characterized by vicariance as well as introgression across typical biogeographic barriers in Northern Australia and New Guinea. Specifically, we infer reticulate evolution around a triad of transient barriers to gene flow between Northern Australia (KP and TE) and New Guinea (PNG) during the Pleistocene, such that introgression occurred between

FIGURE 8 Diversity, differentiation and introgression statistics across regions of the neo-Z and Chr1A. (a) π in nonoverlapping 50 kbp windows, averaged across populations, for the new PAR and recombination suppressed (RS) portions of the added-Z as well as the ancestral-Z-PAR, the ancestral-Z and Chr1A. Outlier points are excluded in (a) but included in (e), which shows windowed π across the chromosomes, as well as a loess smoothed curve (smoothing parameter = 0.1). (b) F_{ST} in nonoverlapping 50 kbp windows shown for the most and least divergent population pairs (KP-EC and KP-TE, respectively), also shown in (g) for all population pairs as loess smoothed curves (smoothing parameter = 0.2). (f) d_{XY} similarly represented as loess smoothed curves. (c, d) The introgression statistic (f_{dM}), summarized across genomic regions, from two topology tests that supported genome-wide introgression (Figure 3); and (h, i) f_d from those topologies, shown in the legend, in nonoverlapping windows of 3000 SNPs with step size of 1000 SNPs between windows. The neo-Z was studied with Scaffold_430 (ONT-Flye-medaka-v1 assembly), representing the ancestral-Z portion of the neo-Z (51.6 Mbp, 70% of zebra finch Z (Figure S1) and contig 4 (ONT-addedZ-v2 assembly), representing most of the added-Z. Contigs from Chr1A (scaffold_334 segments 0 and 1, and contig_1888 from ONT-Flye-medaka-v1) are aligned here according to synteny with zebra finch (bTaeGut1.4.pr, coordinates reversed), which would imply a centromere in the vicinity of 11.6 Mbp (Knief & Forstmeier, 2016).

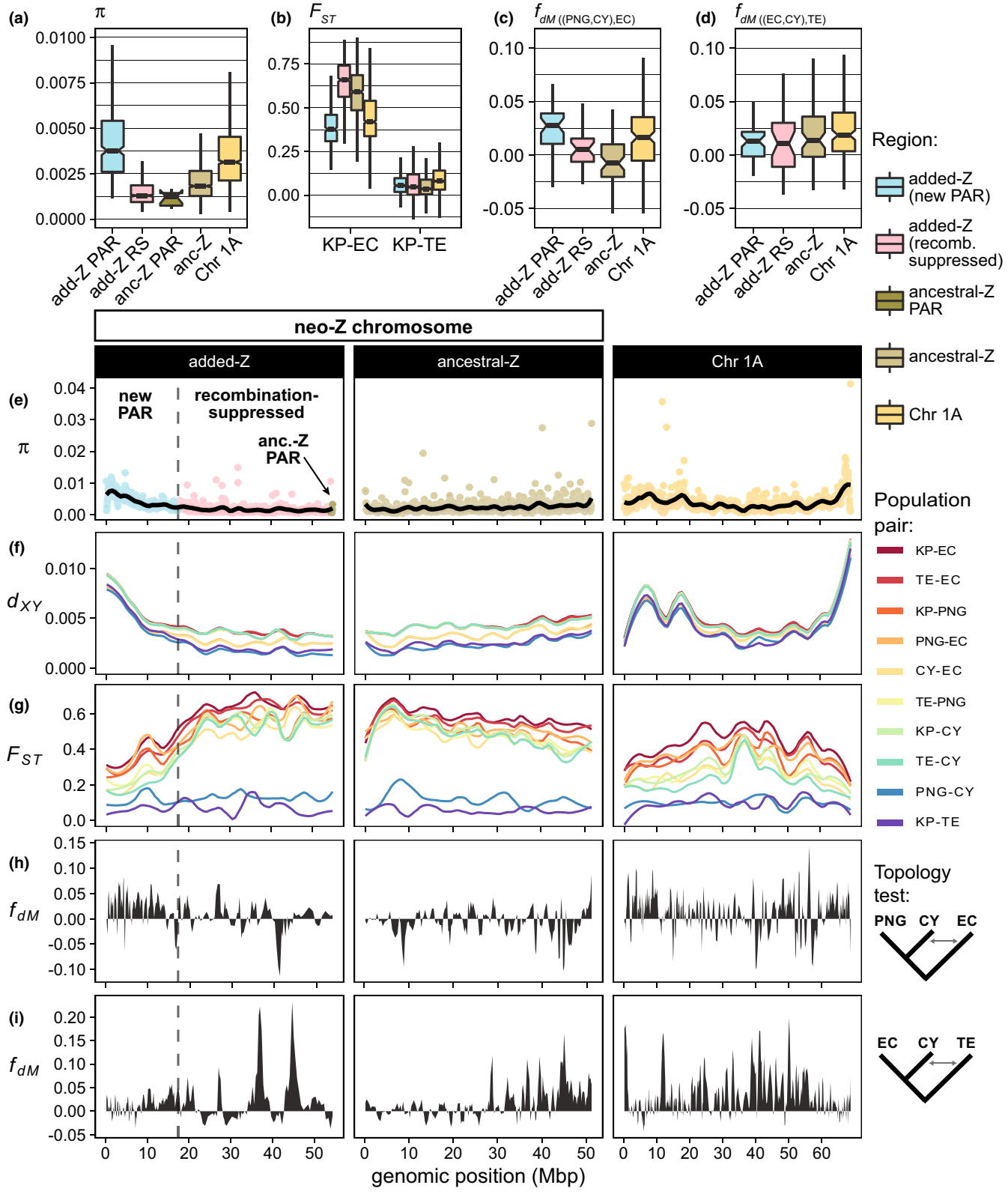

populations that first diverged across the Carpentarian Barrier and apparently then interbred on the Arafura Shelf during recent glacial maxima. Results from tests for unbalanced allele sharing among populations (Figures 3 and 9; Tables S5 and S6), together with estimates of divergence time and historical sea level data (Figures 1d and S3), support a scenario of gene flow between PNG and TE (potentially also KP) via the Arafura Shelf more recently than the divergence between PNG and CY that likely occurred across the Torres Strait. If the PNG-CY divergence occurred following the ~130 ka inundation of the Torres Strait, as opposed to the most recent inundation (~7 ka), then there was a window of approximately 60 ka where the PNG population (*griseigularis*) likely

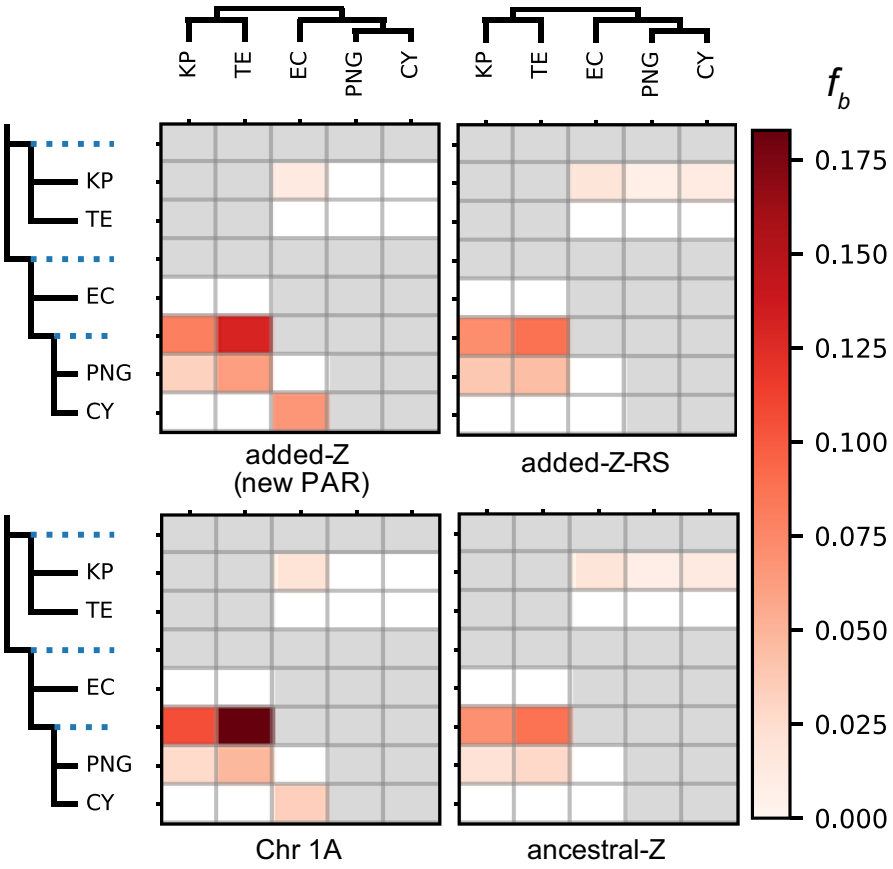

FIGURE 9 The fbranch statistic (f_b) shows excess allele sharing between branches (including internal branches) labelled on the *y* axis and populations labelled on the *x*-axis. The colour scale is consistent across plots for different genomic regions shown.

had contact with subspecies *albipennis* across the Arafura Shelf, which was at that time exposed by sea levels 55 m or more below present levels (Figure S3). Given that the Arafura Shelf is thought to have been covered by savannah woodlands and grasslands when exposed (Hope et al., 2004; Kearns et al., 2014), it is plausible that *E. cyanotis* populations came into contact across this route as well as the Torres Strait land bridge, which was exposed by levels 15 m or more below present levels (Figures 1d and S3). Ancient Lake Carpentaria is thought to have been filled with fresh water from 12 to 36 ka, as well as during earlier glacial maxima, which may have provided a ring of suitable habitat around its shoreline (Chivas et al., 2001; Reeves et al., 2007). Secondary contact between *griseigularis* and *albipennis* may have occurred around the entire perimeter of Lake Carpentaria, although our finding of more extensive allele sharing between TE and PNG than CY and TE implies that the more recent secondary contact primarily occurred across the Arafura Shelf, despite the original split within *E. cyanotis* occurring across the Carpentarian Barrier.

There are two main caveats of our approach for estimating divergence times. First, the model assumption of clean population splits without subsequent gene flow (Bryant et al., 2012) is not met in *E. cyanotis* (Figure 3). Evidence of gene flow presented here implies an increased incidence of recent coalescent events, which may lead to underestimation of divergence times. Second, the only available prior for divergence in this species was derived from the coalescence time of mtDNA (Toon et al., 2010), which is expected to overestimate actual population divergence times (Arbogast et al., 2002). Nevertheless, our estimates are useful in ascertaining the Pleistocene and potentially Holocene diversification of *E. cyanotis*.

Spatial patterns in genetic variation across *E. cyanotis* populations are consistent with a history of gene flow across a network of populations (Duncan et al., 2015; Eckert et al., 2008). This suggestion arises because we find that populations better-connected to others by Pleistocene bridges display greater genome-wide diversity (Figure 2). For example, TE and CY display relatively high π and both are "adjacent" to three other populations, assuming connectivity across all potential bridges, including across the Arafura Sea (Figure 2). By contrast, KP and EC are each "adjacent" to only one other population and have the lowest levels of π – substantially lower in EC – consistent with genetic isolation and population contraction. Elevated genome-wide Tajima's *D* for KP, PNG and EC also suggest that these peripheral populations underwent recent contraction (Tajima, 1989), whereas TE and CY appear to be at mutation-drift equilibrium, with Tajima's *D* values close to 0 (Figure 2b; Table S7). Altogether these results underscore that *E. cyanotis* is best thought of as one species unit despite genetic and phenotypic differentiation. That genetic diversity within species diminishes from range core to periphery is documented across a wide range of taxa and geographic regions and is consistent with population genetic theory (Eckert et al., 2008; Hoffmann & Blows, 1994; Soulé, 1973). Future studies should test the generality of this spatial genetic pattern for Autralo-Papuan taxa because consistent spatial patterns in standing variation across codistributed species may influence how

communities respond to global change, aiding conservation efforts (Ewart et al., 2020; Kelly & Phillips, 2016; Lai et al., 2019; Ralls et al., 2018).

To our knowledge, this study is the first to comprehensively test the hypothesis of introgression across the Arafura Shelf using genome-wide SNPs from whole-genome resequencing (Joseph, Bishop, et al., 2019; Joseph, Dolman, et al., 2019; Kearns et al., 2014), although several studies have investigated patterns of gene flow in this region with other data types, especially mtDNA and RADseq (Andersen et al., 2021; Dorrington et al., 2020; Edwards, 1993a; Joseph, Bishop, et al., 2019; Kearns et al., 2011, 2014; Lamb et al., 2019; Peñalba et al., 2019; Toon et al., 2017). Species histories of other Australo-Papuan taxa might also be shaped by reticulate evolution around the ancient Lake Carpentaria. Our sampling strategy was focused more on determining the existence of gene flow between major areas of endemism rather than measuring rates of gene flow or nonequilibrium demographic events. Future studies to determine taxon-specific histories in this region would benefit from bolstering the number of individuals sampled to test more complex demographic scenarios (reviewed in Beichman et al., 2018). Additionally, sampling from island populations in the Arafura Sea such as the Tiwi and Aru Islands may provide valuable insights into the ancestry of populations that existed on the Arafura Shelf when it was last exposed (Draffan et al., 1983; Edwards, 1993b). Future comparative phylogeographic studies in this region may test theoretical predictions on the time to speciation in three divergent populations compared to two (Peñalba et al., 2019; Yamaguchi & Iwasa, 2017).

4.2 | Evidence for neo-sex chromosomes and fusion scenarios

We present evidence for a major chromosomal rearrangement in *E. cyanotis* featuring translocation from Chr5 to the ancestral PAR of the Z chromosome, based on two independent de novo genome assemblies and population resequencing data. This discovery was made independently of and before we became aware of a similar finding by Sardell (2016) of a neo-sex chromosome in *Myzomela* honeyeaters. Our finding that male-to-female read coverage did not clearly separate sex chromosome-linked scaffolds highlights the need for additional bioinformatic steps to locate sex-linked sequence in organisms where sex chromosomes may vary from homomorphic to heteromorphic (Palmer et al., 2019; Webster et al., 2019). In our case, the large difference in SNP density between males and females flagged a portion of the added-Z as recombination-suppressed and therefore distinct from autosomal sequence (Figures 4 and S8). We additionally relied on synteny mapping with chromosome-level genome assemblies from zebra finch and superb fairywren to determine that scaffolds exhibiting sex-differences in SNP density, but not read coverage, are all homologous to Chr5. Our long-read assembly of the added-Z region strengthens key findings from the earlier assembly: first, that the added portion of the Z, homologous to Chr5, is physically linked to a large new PAR region, and second, that the added-Z is physically linked to a 380 kbp portion of the PAR on the ancestral-Z chromosome.

Our long-read genomic data suggests that a large portion of the putative q-arm of ancestral Chr5 (zebra finch nomenclature) has fused with the ancestral-Z at the PAR end (Figure 6). However, we hypothesize that the ancestral Chr5 centromere did not fuse with the ancestral-Z, because dicentric chromosomes are not as stable or common, although they can in some cases exist stably through inactivation of one of the centromeres (Stimpson et al., 2012). Because we know that at least 55 Mbp of Chr5 fused to Z (Figure 6), the remaining questions are: (i) what is the nature of fusion and degeneration of the other haplotype, which by definition has become an added-W (Beukeboom & Perrin, 2014), and (ii) is the remainder of Chr5 also linked to the neo-Z, or is it now a reduced autosome? Our data cannot yet answer these questions, but double fusions involving the neo-sex chromosomes have been previously documented in the Sylvioidea (sensu Sigeman, 2021 and Alström et al., 2014) neo-sex chromosome system (Sigeman et al., 2019, 2021) and a Chr5-W fusion is likely in larks due to cytogenetic evidence of highly enlarged W chromosomes alongside the enlarged neo-Z (Bulatova, 1981; Sigeman et al., 2019). In such a double fusion scenario, whether fusion with the Z or W would preferentially occur first is not yet clear, however a sequential series of events rather than a simultaneous double fusion seems more biologically plausible. These kinds of rearrangements can potentially lead to PAR enlargement or turnover, where the ancestral PAR ceases to recombine and facilitate pairing during meiosis (Smeds et al., 2014). In *E. cyanotis*, PAR turnover has potentially occurred because the ancestral PAR is now recombination-suppressed, which we infer because it exhibits higher female:male SNP density than expected for a recombining region. It is possible that contig 14 and scaffold 13 in the ONT-addedZ-v2 long-read assembly are part the new PAR, although this might involve additional rearrangement of material from one end of the chromosome to the other, as well as a dicentric neo-Z, which currently seems improbable. All these scenarios need to be further examined cytogenetically.

4.3 | Phylogenetic history of the neo-sex chromosome system in honeyeaters

Viewed in a phylogenetic context, comparing our *E. cyanotis* assemblies to species with PAR identified a priori and to those with known Chr5 translocations bolsters our working hypothesis that Chr5 translocated to the PAR end of Z (Figure 6; Supporting Information). In zebra finch (bTaeGut2.pat.W.v2 and bTaeGut1.4.pri) and collared flycatcher (*Ficedula albicollis*; FicAlb1.5), the location of the PAR was identified previously (Ponnikas et al., 2022; Smeds et al., 2014). The Eurasian skylark, part of the parvorder Sylvioidea possessing the Chr4A translocation to Z/W, was also known to have additional translocations involving Chr5 and Chr3 (Dierickx et al., 2020; Sigeman et al., 2019). Finally, the horned lark was suspected to have these translocations based on cytogenetic evidence, although there

was no signature of recombination suppression on Chr5 in the sampled subspecies (*Eremophila alpestris flava*) from Sweden (Sigeman et al., 2019). The barn swallow, like the larks, is also a member of Sylvioidea, but does not possess this additional translocation involving Chr5. As expected, in barn swallow, zebra finch, collared flycatcher, and superb fairywren, the ancestral PAR assembles separately from Chr5. The fact that the same region on zebra finch Chr5 has fused convergently to the Z-PAR in larks and *E. cyanotis* is intriguing and suggests that this part of the avian genome is prone to rearrangements involving the ancestral sex chromosomes, at least in songbirds.

There are several reasons why this particular region of avian Chr5 may be prone to fusion with the sex chromosomes. One possibility is the presence of similar or shared repeats at the end of the Chr5 long arm and in the telomeric or subtelomeric region of the Z-PAR, leading to interchromosomal rearrangements due to nonallelic homologous recombination events (Gu et al., 2008). Female meiotic drive can also play a role in the formation of neo-sex chromosomes if fused chromosomes involving Chr5 and Z/W are preferentially transmitted to the egg rather than the polar bodies (Yoshida & Kitano, 2012). Centromeric drive has primarily been considered as a mechanism in this context, although telomeres also have the potential to cause segregation distortion during meiosis (Axelsson et al., 2010). In birds, both autosome-Z and autosome-W fusions could potentially be influenced by female meiotic drive since females are the heterogametic sex. If loci involved in sexual traits are enriched on Chr5 in honeyeaters and larks, it could also be adaptive for Chr5 to translocate to the sex chromosomes, since these types of loci are generally under sexually antagonistic selection. A translocation would enable male-beneficial alleles on Chr5 to be in linkage disequilibrium (LD) with the Z (male-biased transmission) and female-beneficial alleles to be in LD with the W (female-limited transmission), thus resolving or reducing sexual antagonism (Matsumoto & Kitano, 2016). Autosomal fusion (whether Chr5 or otherwise) with the ancestral PAR might also be adaptive if the ancestral PAR becomes so small that Z-W pairing during meiosis is compromised, necessitating PAR enlargement or turnover (Blackmon & Demuth, 2015). These will be fruitful avenues to explore in future studies.

Recent genome assemblies in the Meliphagoidea (sensu Marki et al., 2017), the larger clade to which honeyeaters (Meliphagidae) also belong, present clues – and further mystery – about the origin of neo-Z chromosomes detected in *E. cyanotis* (this study) and *Myzomela* (Sardell, 2016). Assemblies from *Malurus* (Peñalba et al., 2020) and *Lichenostomus* (Robledo-Ruiz et al., 2022) show the rearrangement is absent in these taxa. Together, these findings imply independent Chr5-Z fusions in ancestors of *Entomyzon* and *Myzomela*, or alternatively a loss in the lineage leading to *Lichenostomus*, according to a recent phylogenetic analysis (Andersen et al., 2019) based on a concatenated supermatrix of nuclear-genome-wide ultraconserved elements (UCEs), which placed *Myzomela* outside a clade containing *Entomyzon* and *Lichenostomus*. However, phylogenies more heavily reliant on mtDNA markers (Joseph et al., 2014; Marki et al., 2017), place *Lichenostomus* outside of the clade containing both lineages currently known to possess this rearrangement. Therefore, the most parsimonious scenario of a single Chr5-Z fusion in the *Entomyzon-Myzomela* ancestor contradicts the UCE-based phylogeny (Andersen et al., 2019) and aligns with mtDNA-based phylogenies (Joseph et al., 2014; Marki et al., 2017). These observations call for more in-depth phylogenomic work to understand the origins and consequences of neo-sex chromosomes that may occur in more than half of the ~190 honeyeater species.

4.4 | Divergence and introgression landscape of the neo-Z chromosome

The importance of sex chromosomes in speciation is well known (Coyne & Orr, 2004), yet few studies have characterized the genomic divergence landscape across neo-sex chromosomes in ZW systems with some recent exceptions (Mongue et al., 2021; Talla et al., 2020). The formation of large neo-Z chromosomes potentially changes the course of genome evolution because of the sex linkage of genes en masse, recombination suppression and associated changes in linkage and the efficacy of selection (Bachtrog et al., 2011; Shakya et al., 2022). In addition, the formation of new PARs may initiate recombination hotspots in those regions, as PARs typically display elevated recombination compared to genome-wide rates (Janes et al., 2009; Otto et al., 2011). The enlarged neo-Z chromosome found in *E. cyanotis*, combined with the history of reticulate evolution in the species, presents a new opportunity to explore the genomic landscape of population divergence.

Our results portray a genomic divergence landscape on the *E. cyanotis* neo-Z chromosome that, at coarse resolution, is likely shaped by differences in recombination along the chromosome and the increased susceptibility to introgression for recombination hotspots (Figure 8). Diversity (π), and inversely F_{ST}, varies along the neo-Z in accordance with expectations for sequence with Z-W recombination suppression (Charlesworth et al., 1987). However, the neo-Z diversity landscape *E. cyanotis* is yet more complex. The added RS portion of the neo-Z displays reduced π by a factor of 0.71 and faster population genetic differentiation (higher F_{ST}) compared with the ancestral-Z (Figure 8). Yet, the new PAR on average shows elevated π by a factor of 1.16 and reduced differentiation compared to autosomes (Figure 8). In general, d_{XY} is high where F_{ST} is low (Figure 8f,g), which can occur when migration is high during divergence (Cruickshank & Hahn, 2014). We also found stronger evidence for recent introgression on the new PAR than on Chr1A between populations where no signal of introgression was evident on the sex-linked sequence (Figure 8h). Together these results suggest the new PAR in *E. cyanotis* may be a recombination hotspot, consistent with other PARs (Otto et al., 2011), and may thus also be particularly susceptible to introgression (Martin et al., 2019). Similarly, the recombining PAR end of the added portion of the neo-X chromosome in Japan Sea sticklebacks also exhibits a signature of introgression, but it is localized to a small region (Ravinet et al., 2021), even though much of the added portion is recombining (Yoshida et al., 2017).

We found that the genomic signal of recent and ancient introgression scenarios, from tests of imbalanced allele sharing, is variable across the neo-Z. Recent gene flow between subspecies *E. c. griseigularis* in CY and *E. c. cyanotis*, corresponding with a noted hybrid zone (Schodde & Mason, 1999; Figure 1), is evident on the autosomes and the new PAR, but is highly restricted on RS portions of the neo-Z, particularly the added portion (Figures 8c and 9). However, there is no difference between the new PAR and RS portions of the neo-Z in the signal for ancient introgression hypothesized across the Arafura Shelf during Pleistocene glacial maxima (Figure 8d). Depletion of introgression on sex chromosomes is expected to occur, in part, due to the faster rate of accumulation of hybrid incompatibilities compared to autosomes (Hooper et al., 2019; Maheshwari & Barbash, 2011; Martin et al., 2013). Therefore, one possibility to explain the lack of expected variation in evidence for ancient introgression across the neo-Z is that Pleistocene *E. cyanotis* populations were, overall, less diverged compared to present-day populations, such that putative incompatibility loci historically mattered less.

Whereas theoretical expectations of diversity on sex-linked compared to autosomal sequence provides a lens for comparing the evolutionary processes acting on the added-Z and ancestral-Z (Bachtrog et al., 2011; Charlesworth et al., 1987; Pool & Nielsen, 2007), there is little consistency among studied neo-Z systems (Wilson Sayres, 2018). In *E. cyanotis*, reduced π on the added-Z-RS relative to the ancestral-Z is consistent with a stronger role of linked selection or recombination suppression on the added-Z-RS. In either case, the pattern conflicts with that reported in the great reed warbler (*Acrocephalus arundinaceus*), where an added-Z shows even higher genetic diversity than autosomes (Sigeman et al., 2021). A simple explanation for this discrepancy may be related to the position of added Z relative to telomeres, because telomeres tend to have higher recombination rates than central regions of chromosomes (Backstrom et al., 2010; Peñalba et al., 2020). The reed warbler neo-Z involves a relatively small fusion, 9.6 Mbp, with no new PAR associated with it, at the opposite end of the ancestral-Z to the *E. cyanotis* neo-Z. Similarly, in the monarch butterfly neo-Z, genetic diversity in the added-portion is much higher than the ancestral-portion and approaches or is equal to that in the autosomes, depending on the metric (Mongue et al., 2021). In the eastern yellow robin (*Eopsaltria australis*), another Australian songbird with neo-sex chromosomes involving Chr1A (Gan et al., 2019), a region of reduced divsersity within the added portion has been attributed to a recent selective sweep around a cluster of genes involved in mitochondrial coevolution (Gan et al., 2019; Morales et al., 2018). Adaptive evolution could also shape the divergence landscape on the added-Z of *E. cyanotis*, although avian Z chromosomes are also susceptible to enhanced drift relative to autosomes (Hayes et al., 2020; Mank et al., 2010;Shakya et al., 2022). Too few surveys of genetic diversity and other statistics along neo-sex chromosomes in lineages with ZW systems are available to adequately address these different patterns.

Although differences in population genetic statistics along the neo-Z chromosome appear substantial in Figure 8a, we also noted qualitatively similar variation along Chr1A, with elevated diversity and reduced differentiation towards the telomeres (Figure 8e–g), consistent with results for zebra finch (Backstrom et al., 2010). Thus, an alternate interpretation of our results is that patterns of elevated diversity, reduced differentiation and increased introgression on the new PAR are a result of its proximity to the telomere, rather than for being a PAR per se. By similar reasoning, the reduced diversity on the added-Z relative to the ancestral-Z may be a product of its central position in the neo-Z chromosome, rather than an outcome of linked selection as in the eastern yellow robin (Morales et al., 2018). Further analyses are required to distinguish among these hypotheses, but, regardless, long-read sequencing is likely to play an important role in testing them.

4.5 | Conclusions

We present one of the first whole genome phylogeographic surveys of an Australo-Papuan songbird. We inferred multiple instances of introgressive hybridization including ancient gene flow between New Guinea and the north-west of mainland Australia despite a deepest divergence in this species across the Carpentarian Barrier separating subspecies in north-western from eastern Australia. We showed that spatial patterns in genetic diversity are consistent with Pleistocene divergence and convergence across well-known biogeographic barriers, which may be common in co-distributed taxa. Long-read sequencing was instrumental to characterize a neo-Z chromosome, hitherto unknown in this species, that we infer may be shared across honeyeaters; and a parallel translocation in Sylvioidea points to a region of Chr5 as potentially predisposed to the occurrence of this. *Entomyzon cyanotis* population resequencing data mapped to the neo-Z showed microevolutionary consequences of this translocation including a transformed recombination landscape for the affected autosome. Consequences for the recombination suppressed (sex-linked) portion include extremely reduced diversity and resistance to introgression, even compared to the ancestral-Z for which these characteristics are expected. While consequences for the new PAR include increased diversity and patterns of allele sharing between nonsister populations consistent with increased porosity to gene flow compared to autosomes. Our case study shows how the combination of long-read sequencing, for resolving chromosomal rearrangements, with shotgun resequencing across populations can bring synergistic insights for phylogeography and genome evolution.

AUTHOR CONTRIBUTIONS

Scott V. Edwards and John T. Burley conceived of the project; John T. Burley, Sophia C. M. Orzechowski and Simon Yung Wa Sin collected data; John T. Burley and Sophia C. M. Orzechowski analysed data; John T. Burley, Sophia C. M. Orzechowski and Scott V. Edwards wrote the manuscript.

ACKNOWLEDGEMENTS

We thank all permit-granting agencies in Australia and Papua New Guinea for support of this work. We are grateful to Alex Drew, Ian Mason, Chris Wilson and Leo Joseph of the CSIRO Australian National Wildlife Collection (grid.510155.5) for collection of the PNG samples and for use of other ANWC samples, and to the University of Washington Burke Museum, and the University of Kansas Biodiversity Institute for also providing tissue samples used in these analyses. Jeremiah Trimble and Breda Zimkus assisted with tissue samples in the Museum of Comparative Zoology. We thank Claire Reardon Bailey Hartmann from the Bauer Core Sequencing facility at Harvard University for her assistance with PromethION/MinION sequencing; Tim Sackton and Danielle Khost for helpful feedback and discussion regarding the refinement of the added-Z assembly; Allison Shultz, Alison Cloutier, Phil Grayson, Gustavo Bravo, Tim Sackton and Sangeet Lamichhaney for helpful bioinformatics advice; Desi Petkova and Katherine Silliman for assistance with EEMS; Niclas Backström for helpful feedback on an earlier version of this work; and Bengt Hansson and Hanna Sigeman for helpful discussion regarding the fusion scenario with the ancestral PAR. We thank Leo Joseph, David Peede, Christine Muir and the laboratories of Albert Uy and Daren Presgraves, as well as three anonymous reviewers, for valuable manuscript suggestions. This study was supported by a MEME fellowship to JTB and Harvard University.

CONFLICT OF INTERESTS

The authors have no conflicts of interest to disclose.

DATA AVAILABILITY AND BENEFIT-SHARING STATEMENT

This Whole Genome Shotgun project has been deposited at DDBJ/ENA/GenBank under the accession NHZT00000000 and NCBI BioProject PRJNA387313. The version of the short-read assembly described in this study is version NHZT01000000. The ONT-Flye-Medaka-v1 long-read assembly with ONT-addedZ-v2 inserted into it has been deposited under the accession JAKEPQ000000000 in NCBI BioProject PRJNA387313. All whole genome shotgun resequencing and long-read data have been deposited to NCBI under BioProject PRJNA387313 (https://www.ncbi.nlm.nih.gov/sra/PRJNA387313). Other data sets are deposited in the Dryad at https://doi.org/10.5061/dryad.7pvmcvdvg. Analysis scripts can be found at https://github.com/johnburley3000/genomics_Entomyzon.

OPEN RESEARCH BADGES

This article has earned an Open Data badge for making publicly available the digitally-shareable data necessary to reproduce the reported results. The data is available at https://doi.org/10.5061/dryad.7pvmcvdvg.

ORCID

Sophia C. M. Orzechowski https://orcid.org/0000-0002-6746-6388
Simon Yung Wa Sin https://orcid.org/0000-0003-2484-2897
Scott V. Edwards https://orcid.org/0000-0003-2535-6217

REFERENCES

Alström, P., Hooper, D. M., Liu, Y., Olsson, U., Mohan, D., Gelang, M., Le Manh, H., Zhao, J., Lei, F., & Price, T. D. (2014). Discovery of a relict lineage and monotypic family of passerine birds. *Biology Letters*, *10*(3), 20131067. https://doi.org/10.1098/rsbl.2013.1067

Andersen, M. J., McCullough, J. M., Friedman, N. R., Peterson, A. T., Moyle, R. G., Joseph, L., & Nyári, Á. S. (2019). Ultraconserved elements resolve genus-level relationships in a major Australasian bird radiation (Aves: Meliphagidae). *Emu - Austral Ornithology*, *119*(3), 218–232. https://doi.org/10.1080/01584197.2019.1595662

Andersen, M. J., McCullough, J. M., Gyllenhaal, E. F., Mapel, X. M., Haryoko, T., Jønsson, K. A., & Joseph, L. (2021). Complex histories of gene flow and a mitochondrial capture event in a nonsister pair of birds. *Molecular Ecology*, *30*(9), 2087–2103. https://doi.org/10.1111/mec.15856

Ankenbrand, M. J., Hohlfeld, S., Hackl, T., & Förster, F. (2017). AliTV—Interactive visualization of whole genome comparisons. *PeerJ Computer Science*, *3*, e116. https://doi.org/10.7717/peerj-cs.116

Arbogast, B. S., Edwards, S. V., Wakeley, J., Beerli, P., & Slowinski, J. B. (2002). Estimating divergence times from molecular data on phylogenetic and population genetic timescales. *Annual Review of Ecology and Systematics*, *33*(1), 707–740. https://doi.org/10.1146/annurev.ecolsys.33.010802.150500

Axelsson, E., Albrechtsen, A., Van, A. P., Li, L., Megens, H. J., Vereijken, A. L. J., Crooijmans, R. P. M. A., Groenen, M. A. M., Ellegren, H., Willerslev, E., & Nielsen, R. (2010). Segregation distortion in chicken and the evolutionary consequences of female meiotic drive in birds. *Heredity*, *105*(3), 290–298. https://doi.org/10.1038/hdy.2009.193

Bachtrog, D., Kirkpatrick, M., Mank, J. E., McDaniel, S. F., Pires, J. C., Rice, W., & Valenzuela, N. (2011). Are all sex chromosomes created equal? *Trends in Genetics*, *27*(9), 350–357. https://doi.org/10.1016/j.tig.2011.05.005

Backstrom, N., Forstmeier, W., Schielzeth, H., Mellenius, H., Nam, K., Bolund, E., Webster, M. T., Ost, T., Schneider, M., Kempenaers, B., & Ellegren, H. (2010). The recombination landscape of the zebra finch *Taeniopygia guttata* genome. *Genome Research*, *20*(4), 485–495. https://doi.org/10.1101/gr.101410.109

Bakker, V. J., Finkelstein, M. E., D'Elia, J., Doak, D. F., & Kirkland, S. (2022). Genetically based demographic reconstructions require careful consideration of generation time. *Current Biology*, *32*, R356–R357.

Beichman, A. C., Huerta-Sanchez, E., & Lohmueller, K. E. (2018). Using genomic data to infer historic population dynamics of nonmodel organisms. *Annual Review of Ecology, Evolution, and Systematics*, *49*(1), 433–456. https://doi.org/10.1146/annurev-ecolsys-110617-062431

Beukeboom, L. W., & Perrin, N. (2014). *The evolution of sex determination* (1st ed.). Oxford University Press.

Beyter, D., Ingimundardottir, H., Oddsson, A., Eggertsson, H. P., Bjornsson, E., Jonsson, H., Atlason, B. A., Kristmundsdottir, S., Mehringer, S., Hardarson, M. T., Gudjonsson, S. A., Magnusdottir, D. N., Jonasdottir, A., Jonasdottir, A., Kristjansson, R. P., Sverrisson, S. T., Holley, G., Palsson, G., Stefansson, O. A., … Stefansson, K. (2020). Long read sequencing of 3,622 Icelanders provides insight into the role of structural variants in human diseases and other traits. *bioRxiv*. https://doi.org/10.1101/848366

Blackmon, H., & Demuth, J. P. (2015). The fragile Y hypothesis: Y chromosome aneuploidy as a selective pressure in sex chromosome and meiotic mechanism evolution. *BioEssays: News and Reviews in Molecular, Cellular and Developmental Biology*, *37*(9), 942–950. https://doi.org/10.1002/bies.201500040

Bowman, D. M. J. S., Brown, G. K., Braby, M. F., Brown, J. R., Cook, L. G., Crisp, M. D., Ford, F., Haberle, S., Hughes, J., Isagi, Y., Joseph, L., McBride, J., Nelson, G., & Ladiges, P. Y. (2010). Biogeography of the Australian monsoon tropics. *Journal of Biogeography*, *37*(2), 201–216. https://doi.org/10.1111/j.1365-2699.2009.02210.x

Bracewell, R. R., Bentz, B. J., Sullivan, B. T., & Good, J. M. (2017). Rapid neo-sex chromosome evolution and incipient speciation in a major forest pest. *Nature Communications*, *8*(1), 1593. https://doi.org/10.1038/s41467-017-01761-4

Bravo, G. A., Schmitt, C. J., & Edwards, S. V. (2021). What have we learned from the first 500 avian genomes? *Annual Review of Ecology, Evolution, and Systematics*, *52*, 611–639.

Brito, P. H., & Edwards, S. V. (2009). Multilocus phylogeography and phylogenetics using sequence-based markers. *Genetica*, *135*, 439–455.

Bryant, D., Bouckaert, R., Felsenstein, J., Rosenberg, N. A., & RoyChoudhury, A. (2012). Inferring species trees directly from biallelic genetic markers: Bypassing gene trees in a full coalescent analysis. *Molecular Biology and Evolution*, *29*(8), 1917–1932. https://doi.org/10.1093/molbev/mss086

Bryant, L. M., & Krosch, M. N. (2016). Lines in the land: A review of evidence for eastern Australia's major biogeographical barriers to closed forest taxa. *Biological Journal of the Linnean Society*, *119*(2), 238–264. https://doi.org/10.1111/bij.12821

Buckner, J. C., Sanders, R. C., Faircloth, B. C., & Chakrabarty, P. (2021). The critical importance of vouchers in genomics. *eLife*, *10*, e68264. https://doi.org/10.7554/eLife.68264

Bulatova, N. (1981). A comparative karyological study of passerine birds. *Acta Scientiarum Naturalium Academiae Scientiarum Bohemicae*, *15*, 1–44.

Charlesworth, B., Coyne, J. A., & Barton, N. H. (1987). The relative rates of evolution of sex chromosomes and autosomes. *The American Naturalist*, *130*(1), 113–146.

Chivas, A. R., García, A., van der Kaars, S., Couapel, M. J. J., Holt, S., Reeves, J. M., Wheeler, D. J., Switzer, A. D., Murray-Wallace, C. V., Banerjee, D., Price, D. M., Wang, S. X., Pearson, G., Edgar, N. T., Beaufort, L., De Deckker, P., Lawson, E., & Cecil, C. B. (2001). Sea-level and environmental changes since the last interglacial in the Gulf of Carpentaria, Australia: An overview. *Quaternary International*, *83–85*, 19–46. https://doi.org/10.1016/S1040-6182(01)00029-5

Coyne, J. A., & Orr, H. A. (2004). *Speciation*. Oxford University Press.

Cracraft, J. (1986). Origin and evolution of continental biotas: Speciation and historical congruence within the Australian avifauna. *Evolution*, *40*(5), 977–996. https://doi.org/10.1111/j.1558-5646.1986.tb00566.x

Cruickshank, T. E., & Hahn, M. W. (2014). Reanalysis suggests that genomic islands of speciation are due to reduced diversity, not reduced gene flow. *Molecular Ecology*, *23*(13), 3133–3157. https://doi.org/10.1111/mec.12796

Cutter, A. D. (2013). Integrating phylogenetics, phylogeography and population genetics through genomes and evolutionary theory. *Molecular Phylogenetics and Evolution*, *69*(3), 1172–1185. https://doi.org/10.1016/j.ympev.2013.06.006

de Boer, B., Lourens, L. J., & van de Wal, R. S. W. (2014). Persistent 400,000-year variability of Antarctic ice volume and the carbon cycle is revealed throughout the Plio-Pleistocene. *Nature Communications*, *5*(1), 2999. https://doi.org/10.1038/ncomms3999

De Coster, W., Weissensteiner, M. H., & Sedlazeck, F. J. (2021). Towards population-scale long-read sequencing. *Nature Reviews Genetics*, *22*(9), 572–587. https://doi.org/10.1038/s41576-021-00367-3

Dierickx, E. G., Sin, S. Y. W., van Veelen, H. P. J., Brooke, M. L., Liu, Y., Edwards, S. V., & Martin, S. H. (2020). Genetic diversity, demographic history and neo-sex chromosomes in the critically endangered Raso lark. *Proceedings of the Royal Society B: Biological Sciences*, *287*(1922), 20192613. https://doi.org/10.1098/rspb.2019.2613

Dorrington, A., Joseph, L., Hallgren, W., Mason, I., Drew, A., Hughes, J. M., & Schmidt, D. J. (2020). Phylogeography of the blue-winged kookaburra *Dacelo leachii* across tropical northern Australia and New Guinea. *Emu - Austral Ornithology*, *120*(1), 33–45. https://doi.org/10.1080/01584197.2019.1670585

Dos Santos, M. S., Kretschmer, R., Frankl-Vilches, C., Bakker, A., Gahr, M., O'Brien, P. C. M., Ferguson-Smith, M. A., & de Oliveira, E. H. C. (2017). Comparative cytogenetics between two important songbird, models: The zebra finch and the canary. *PLoS One*, *12*(1), e0170997. https://doi.org/10.1371/journal.pone.0170997

Draffan, R. D. W., Garnett, S. T., & Malone, G. J. (1983). Birds of the Torres Strait: An annotated list and biogeographical analysis. *Emu - Austral Ornithology*, *83*(4), 207–234. https://doi.org/10.1071/MU9830207

Duncan, S. I., Crespi, E. J., Mattheus, N. M., & Rissler, L. J. (2015). History matters more when explaining genetic diversity within the context of the core–periphery hypothesis. *Molecular Ecology*, *24*(16), 4323–4336. https://doi.org/10.1111/mec.13315

Durand, E. Y., Patterson, N., Reich, D., & Slatkin, M. (2011). Testing for ancient admixture between closely related populations. *Molecular Biology and Evolution*, *28*(8), 2239–2252. https://doi.org/10.1093/molbev/msr048

Eckert, C. G., Samis, K. E., & Lougheed, S. C. (2008). Genetic variation across species' geographical ranges: The central-marginal hypothesis and beyond. *Molecular Ecology*, *17*(5), 1170–1188. https://doi.org/10.1111/j.1365-294X.2007.03659.x

Edwards, R. D., Crisp, M. D., Cook, D. H., & Cook, L. G. (2017). Congruent biogeographical disjunctions at a continent-wide scale: Quantifying and clarifying the role of biogeographic barriers in the Australian tropics. *PLoS One*, *12*(4), e0174812. https://doi.org/10.1371/journal.pone.0174812

Edwards, S. V. (1993a). Mitochondrial gene genealogy and gene flow among Island and mainland populations of a sedentary songbird, the Grey-crowned babbler (*Pomatostomus temporalis*). *Evolution*, *47*(4), 1118–1137. https://doi.org/10.1111/j.1558-5646.1993.tb02140.x

Edwards, S. V. (1993b). Long-distance gene flow in a cooperative breeder detected in genealogies of mitochondrial DNA sequences. *Proceedings of the Royal Society of London. Series B: Biological Sciences*, *252*(1335), 177–185. https://doi.org/10.1098/rspb.1993.0063

Edwards, S. V., Potter, S., Schmitt, C. J., Bragg, J. G., & Moritz, C. (2016). Reticulation, divergence, and the phylogeography–phylogenetics continuum. *Proceedings of the National Academy of Sciences of the United States of America*, *113*(29), 8025–8032. https://doi.org/10.1073/pnas.1601066113

Edwards, S. V., Robin, V. V., Ferrand, N., & Moritz, C. (2021). The evolution of comparative phylogeography: Putting the geography (and more) into comparative population genomics. *Genome Biology and Evolution*, *14*(1), https://doi.org/10.1093/gbe/evab176

Edwards, S. V., Shultz, A. J., & Campbell-Staton, S. C. (2015). Next-generation sequencing and the expanding domain of phylogeography. *Folia Zoologica*, *64*(3), 187–206. https://doi.org/10.25225/fozo.v64.i3.a2.2015

Ellegren, H. (2010). Evolutionary stasis: The stable chromosomes of birds. *Trends in Ecology & Evolution*, *25*(5), 283–291. https://doi.org/10.1016/j.tree.2009.12.004

Ewart, K. M., Lo, N., Ogden, R., Joseph, L., Ho, S. Y. W., Frankham, G. J., Eldridge, M. D. B., Schodde, R., & Johnson, R. N. (2020). Phylogeography of the iconic Australian red-tailed black-cockatoo (*Calyptorhynchus banksii*) and implications for its conservation.

Heredity, *125*(3), 85–100. https://doi.org/10.1038/s41437-020-0315-y

Fang, B., Merilä, J., Matschiner, M., & Momigliano, P. (2020). Estimating uncertainty in divergence times among three-spined stickleback clades using the multispecies coalescent. *Molecular Phylogenetics and Evolution*, *142*, 106646. https://doi.org/10.1016/j.ympev.2019.106646

Ford, J. (1978). Geographical isolation and morphological and habitat differentiation between birds of the Kimberley and the Northern Territory. *Emu - Austral Ornithology*, *78*(1), 25–35. https://doi.org/10.1071/MU9780025

Ford, J. (1982). Origin, evolution and speciation of birds specialized to mangroves in Australia. *Emu - Austral Ornithology*, *82*(1), 12–23. https://doi.org/10.1071/MU9820012

Fridolfsson, A.-K., & Ellegren, H. (1999). A simple and universal method for molecular sexing of non-ratite birds. *Journal of Avian Biology*, *30*(1), 116–121. https://doi.org/10.2307/3677252

Fumagalli, M., Vieira, F. G., Korneliussen, T. S., Linderoth, T., Huerta-Sánchez, E., Albrechtsen, A., & Nielsen, R. (2013). Quantifying population genetic differentiation from next-generation sequencing data. *Genetics*, *195*(3), 979–992. https://doi.org/10.1534/genetics.113.154740

Fumagalli, M., Vieira, F. G., Linderoth, T., & Nielsen, R. (2014). ngsTools: Methods for population genetics analyses from next-generation sequencing data. *Bioinformatics*, *30*(10), 1486–1487. https://doi.org/10.1093/bioinformatics/btu041

Gan, H. M., Falk, S., Morales, H. E., Austin, C. M., Sunnucks, P., & Pavlova, A. (2019). Genomic evidence of neo-sex chromosomes in the eastern yellow robin. *GigaScience*, *8*(9), 1–10. https://doi.org/10.1093/gigascience/giz111

Gnerre, S., MacCallum, I., Przybylski, D., Ribeiro, F. J., Burton, J. N., Walker, B. J., Sharpe, T., Hall, G., Shea, T. P., Sykes, S., Berlin, A. M., Aird, D., Costello, M., Daza, R., Williams, L., Nicol, R., Gnirke, A., Nusbaum, C., Lander, E. S., & Jaffe, D. B. (2011). High-quality draft assemblies of mammalian genomes from massively parallel sequence data. *Proceedings of the National Academy of Sciences of the United States of America*, *108*(4), 1513–1518. https://doi.org/10.1073/pnas.1017351108

Grabherr, M. G., Russell, P., Meyer, M., Mauceli, E., Alföldi, J., Di Palma, F., & Lindblad-Toh, K. (2010). Genome-wide synteny through highly sensitive sequence alignment: Satsuma. *Bioinformatics*, *26*(9), 1145–1151. https://doi.org/10.1093/bioinformatics/btq102

Grayson, P., Sin, S. Y. W., Sackton, T. B., & Edwards, S. V. (2017). Comparative genomics as a Foundation for Evo-Devo studies in birds. *Methods in Molecular Biology*, *1650*, 11–46. https://doi.org/10.1007/978-1-4939-7216-6_2

Gu, W., Zhang, F., & Lupski, J. R. (2008). Mechanisms for human genomic rearrangements. *PathoGenetics*, *1*(1), Article number: 4. https://doi.org/10.1186/1755-8417-1-4

Guiglielmoni, N., Houtain, A., Derzelle, A., Van Doninck, K., & Flot, J.-F. (2021). Overcoming uncollapsed haplotypes in long-read assemblies of non-model organisms. *BMC Bioinformatics*, *22*(1), 303. https://doi.org/10.1186/s12859-021-04118-3

Harvey, M. G., & Brumfield, R. T. (2015). Genomic variation in a widespread neotropical bird (*Xenops minutus*) reveals divergence, population expansion, and gene flow. *Molecular Phylogenetics and Evolution*, *83*, 305–316. https://doi.org/10.1016/j.ympev.2014.10.023

Hayes, K., Barton, H. J., & Zeng, K. (2020). A study of faster-Z evolution in the great tit (*Parus major*). *Genome Biology and Evolution*, *12*(3), 210–222. https://doi.org/10.1093/gbe/evaa044

Higgins, P. J., del Hoyo, J., Collar, N., Christidis, L., Kirwan, G. M., & Ford, H. (2020). Blue-faced honeyeater (*Entomyzon cyanotis*) version 1.0. In S. M. Billerman, B. K. Keeney, P. G. Rodewald, & T. S. Schulenberg (Eds.), *Birds of the world*. Cornell Lab of Ornithology. https://doi.org/10.2173/bow.blfhon1.01

Hoffmann, A. A., & Blows, M. W. (1994). Species borders: Ecological and evolutionary perspectives. *Trends in Ecology & Evolution*, *9*(6), 223–227. https://doi.org/10.1016/0169-5347(94)90248-8

Hooper, D. M., Griffith, S. C., & Price, T. D. (2019). Sex chromosome inversions enforce reproductive isolation across an avian hybrid zone. *Molecular Ecology*, *28*(6), 1246–1262. https://doi.org/10.1111/mec.14874

Hope, G., Kershaw, A. P., van der Kaars, S., Xiangjun, S., Liew, P.-M., Heusser, L. E., Takahara, H., McGlone, M., Miyoshi, N., & Moss, P. T. (2004). History of vegetation and habitat change in the Austral-Asian region. *Quaternary International*, *118–119*, 103–126. https://doi.org/10.1016/S1040-6182(03)00133-2

Huang, Y.-T., Liu, P.-Y., & Shih, P.-W. (2021). Homopolish: A method for the removal of systematic errors in nanopore sequencing by homologous polishing. *Genome Biology*, *22*(1), 95. https://doi.org/10.1186/s13059-021-02282-6

Huang, Z., Furo, I., Peona, V., Liu, J., Gomes, A. J. B., Cen, W., Huang, H., Zhang, Y., Chen, D., Ting, X., Chen, Y., Zhang, Q., Yue, Z., Suh, A., de Oliveira, E. H. C., & Xu, L. (2021). *Recurrent chromosome reshuffling and the evolution of neo-sex chromosomes in parrots* (p. 2021.03.08.434498). https://doi.org/10.1101/2021.03.08.434498

Jain, C., Rodriguez-R, L. M., Phillippy, A. M., Konstantinidis, K. T., & Aluru, S. (2018). High throughput ANI analysis of 90K prokaryotic genomes reveals clear species boundaries. *Nature Communications*, *9*(1), https://doi.org/10.1038/s41467-018-07641-9

Janes, D. E., Ezaz, T., Marshall Graves, J. A., & Edwards, S. V. (2009). Recombination and nucleotide diversity in the sex chromosomal Pseudoautosomal region of the emu, *Dromaius novaehollandiae*. *Journal of Heredity*, *100*(2), 125–136. https://doi.org/10.1093/jhered/esn065

Jennings, W. B., & Edwards, S. V. (2005). Speciation history of Australian grass finches (Poephila) inferred from thirty gene trees. *Evolution*, *59*(9), 2033–2047. https://doi.org/10.1554/05-280.1

Jonasson, J., Harkonen, T., Sundqvist, L., Edwards, S. V., & Harding, K. C. (2022). A unifying framework for estimating generation time in age-structured populations: Implications for phylogenetics and conservation biology. *American Naturalist*, *200*, 48–62.

Jones, M. R., & Torgersen, T. (1988). Late quaternary evolution of Lake Carpentaria on the Australia-New Guinea continental shelf. *Australian Journal of Earth Sciences*, *35*(3), 313–324. https://doi.org/10.1080/08120098808729450

Joseph, L., Bishop, K. D., Wilson, C. A., Edwards, S. V., Iova, B., Campbell, C. D., Mason, I., & Drew, A. (2019). A review of evolutionary research on birds of the new Guinean savannas and closely associated habitats of riparian rainforests, mangroves and grasslands. *Emu - Austral Ornithology*, *119*(3), 317–330. https://doi.org/10.1080/01584197.2019.1615844

Joseph, L., Dolman, G., Iova, B., Jønsson, K., Campbell, C. D., Mason, I., & Drew, A. (2019). Aberrantly plumaged orioles from the trans-Fly savannas of New Guinea and their ecological and evolutionary significance. *Emu - Austral Ornithology*, *119*(3), 264–273. https://doi.org/10.1080/01584197.2019.1605831

Joseph, L., Toon, A., Nyári, Á. S., Longmore, N. W., Rowe, K. M. C., Haryoko, T., Trueman, J., & Gardner, J. L. (2014). A new synthesis of the molecular systematics and biogeography of honeyeaters (Passeriformes: Meliphagidae) highlights biogeographical and ecological complexity of a spectacular avian radiation. *Zoologica Scripta*, *43*(3), 235–248. https://doi.org/10.1111/zsc.12049

Kearns, A. M., Joseph, L., Omland, K. E., & Cook, L. G. (2011). Testing the effect of transient Plio-Pleistocene barriers in monsoonal Australo-Papua: Did mangrove habitats maintain genetic connectivity in the black butcherbird? *Molecular Ecology*, *20*(23), 5042–5059. https://doi.org/10.1111/j.1365-294X.2011.05330.x

Kearns, A. M., Joseph, L., Toon, A., & Cook, L. G. (2014). Australia's arid-adapted butcherbirds experienced range expansions during Pleistocene glacial maxima. *Nature Communications*, *5*(1), 1–11. https://doi.org/10.1038/ncomms4994

Keast, A. (1961). Bird speciation on the Australian continent. *Bulletin of the Museum of Comparative Zoology at Harvard College*, *123*, 303–495.

Kelly, E., & Phillips, B. L. (2016). Targeted gene flow for conservation. *Conservation Biology*, *30*(2), 259–267. https://doi.org/10.1111/cobi.12623

Kitano, J., Ross, J. A., Mori, S., Kume, M., Jones, F. C., Chan, Y. F., Absher, D. M., Grimwood, J., Schmutz, J., Myers, R. M., Kingsley, D. M., & Peichel, C. L. (2009). A role for a neo-sex chromosome in stickleback speciation. *Nature*, *461*(7267), 1079–1083. https://doi.org/10.1038/nature08441

Knief, U., & Forstmeier, W. (2016). Mapping centromeres of microchromosomes in the zebra finch (*Taeniopygia guttata*) using half-tetrad analysis. *Chromosoma*, *125*(4), 757–768. https://doi.org/10.1007/s00412-015-0560-7

Kolmogorov, M., Yuan, J., Lin, Y., & Pevzner, P. A. (2019). Assembly of long, error-prone reads using repeat graphs. *Nature Biotechnology*, *37*(5), 540–546. https://doi.org/10.1038/s41587-019-0072-8

Korneliussen, T. S., Albrechtsen, A., & Nielsen, R. (2014). ANGSD: Analysis of next generation sequencing data. *BMC Bioinformatics*, *15*(1), 356. https://doi.org/10.1186/s12859-014-0356-4

Korunes, K. L., & Samuk, K. (2021). Pixy: Unbiased estimation of nucleotide diversity and divergence in the presence of missing data. *Molecular Ecology Resources*, *21*(4), 1359–1368. https://doi.org/10.1111/1755-0998.13326

Lai, Y.-T., Yeung, C. K. L., Omland, K. E., Pang, E.-L., Hao, Y., Liao, B.-Y., Cao, H.-F., Zhang, B.-W., Yeh, C.-F., Hung, C.-M., Hung, H.-Y., Yang, M.-Y., Liang, W., Hsu, Y.-C., Yao, C.-T., Dong, L., Lin, K., & Li, S.-H. (2019). Standing genetic variation as the predominant source for adaptation of a songbird. *Proceedings of the National Academy of Sciences of the United States of America*, *116*(6), 2152–2157. https://doi.org/10.1073/pnas.1813597116

Lamb, A. M., Gonçalves da Silva, A., Joseph, L., Sunnucks, P., & Pavlova, A. (2019). Pleistocene-dated biogeographic barriers drove divergence within the Australo-Papuan region in a sex-specific manner: An example in a widespread Australian songbird. *Heredity*, *123*, 608–621. https://doi.org/10.1038/s41437-019-0206-2

Lamichhaney, S., Han, F., Berglund, J., Wang, C., Almen, M. S., Webster, M. T., Grant, B. R., Grant, P. R., & Andersson, L. (2016). A beak size locus in Darwins finches facilitated character displacement during a drought. *Science*, *352*(6284), 470–474. https://doi.org/10.1126/science.aad8786

Lee, J. Y., & Edwards, S. V. (2008). Divergence across Australia's Carpentarian barrier: Statistical phylogeography of the red-backed fairy wren (*Malurus melanocephalus*). *Evolution*, *62*(12), 3117–3134. https://doi.org/10.1111/j.1558-5646.2008.00543.x

Leroy, T., Anselmetti, Y., Tilak, M.-K., Bérard, S., Csukonyi, L., Gabrielli, M., Scornavacca, C., Milá, B., Thébaud, C., & Nabholz, B. (2019). A bird's white-eye view on neosex chromosome evolution. *bioRxiv*. https://doi.org/10.1101/505610

Li, H. (2018). Minimap2: Pairwise alignment for nucleotide sequences. *Bioinformatics*, *34*(18), 3094–3100. https://doi.org/10.1093/bioinformatics/bty191

Li, H., & Durbin, R. (2009). Fast and accurate short read alignment with Burrows–Wheeler transform. *Bioinformatics*, *25*(14), 1754–1760. https://doi.org/10.1093/bioinformatics/btp324

Li, H., Handsaker, B., Wysoker, A., Fennell, T., Ruan, J., Homer, N., Marth, G., Abecasis, G., Durbin, R., & 1000 Genome Project Data Processing Subgroup. (2009). The sequence alignment/map format and SAMtools. *Bioinformatics*, *25*(16), 2078–2079. https://doi.org/10.1093/bioinformatics/btp352

Lopez, K. A., McDiarmid, C. S., Griffith, S. C., Lovette, I. J., & Hooper, D. M. (2021). Evaluating evidence of mitonuclear incompatibilities with the sex chromosomes in an avian hybrid zone. *Evolution*, *75*(6), 1395–1414. https://doi.org/10.1111/evo.14243

Maheshwari, S., & Barbash, D. A. (2011). The genetics of hybrid incompatibilities. *Annual Review of Genetics*, *45*(1), 331–355. https://doi.org/10.1146/annurev-genet-110410-132514

Malinsky, M., Challis, R. J., Tyers, A. M., Schiffels, S., Terai, Y., Ngatunga, B. P., Miska, E. A., Durbin, R., Genner, M. J., & Turner, G. F. (2015). Genomic islands of speciation separate cichlid ecomorphs in an East African crater lake. *Science*, *350*(6267), 1493–1498. https://doi.org/10.1126/science.aac9927

Malinsky, M., Matschiner, M., & Svardal, H. (2021). Dsuite—Fast D-statistics and related admixture evidence from VCF files. *Molecular Ecology Resources*, *21*(2), 584–595. https://doi.org/10.1111/1755-0998.13265

Malinsky, M., Svardal, H., Tyers, A. M., Miska, E. A., Genner, M. J., Turner, G. F., & Durbin, R. (2018). Whole-genome sequences of Malawi cichlids reveal multiple radiations interconnected by gene flow. *Nature Ecology & Evolution*, *2*(12), 1940–1955. https://doi.org/10.1038/s41559-018-0717-x

Mank, J. E., Nam, K., & Ellegren, H. (2010). Faster-Z evolution is predominantly due to genetic drift. *Molecular Biology and Evolution*, *27*(3), 661–670. https://doi.org/10.1093/molbev/msp282

Marki, P. Z., Jønsson, K. A., Irestedt, M., Nguyen, J. M. T., Rahbek, C., & Fjeldså, J. (2017). Supermatrix phylogeny and biogeography of the Australasian Meliphagides radiation (Aves: Passeriformes). *Molecular Phylogenetics and Evolution*, *107*, 516–529.

Martin, S. H., Dasmahapatra, K. K., Nadeau, N. J., Salazar, C., Walters, J. R., Simpson, F., Blaxter, M., Manica, A., Mallet, J., & Jiggins, C. D. (2013). Genome-wide evidence for speciation with gene flow in *Heliconius* butterflies. *Genome Research*, *23*(11), 1817–1828. https://doi.org/10.1101/gr.159426.113

Martin, S. H., Davey, J. W., & Jiggins, C. D. (2015). Evaluating the use of ABBA–BABA statistics to locate Introgressed loci. *Molecular Biology and Evolution*, *32*(1), 244–257. https://doi.org/10.1093/molbev/msu269

Martin, S. H., Davey, J. W., Salazar, C., & Jiggins, C. D. (2019). Recombination rate variation shapes barriers to introgression across butterfly genomes. *PLoS Biology*, *17*(2), e2006288. https://doi.org/10.1371/journal.pbio.2006288

Martin, S. H., Singh, K. S., Gordon, I. J., Omufwoko, K. S., Collins, S., Warren, I. A., Munby, H., Brattström, O., Traut, W., Martins, D. J., Smith, D. A. S., Jiggins, C. D., Bass, C., & ffrench-Constant, R. H. (2020). Whole-chromosome hitchhiking driven by a male-killing endosymbiont. *PLoS Biology*, *18*(2), e3000610. https://doi.org/10.1371/journal.pbio.3000610

Matsumoto, T., & Kitano, J. (2016). The intricate relationship between sexually antagonistic selection and the evolution of sex chromosome fusions. *Journal of Theoretical Biology*, *404*, 97–108. https://doi.org/10.1016/j.jtbi.2016.05.036

Mayr, E. (1940). Speciation phenomena in birds. *The American Naturalist*, *74*(752), 249–278.

McKenna, A., Hanna, M., Banks, E., Sivachenko, A., Cibulskis, K., Kernytsky, A., Garimella, K., Altshuler, D., Gabriel, S., Daly, M., & DePristo, M. A. (2010). The genome analysis toolkit: A MapReduce framework for analyzing next-generation DNA sequencing data. *Genome Research*, *20*(9), 1297–1303. https://doi.org/10.1101/gr.107524.110

Mongue, A. J., Hansen, M. E., & Walters, J. R. (2021). Support for faster and more adaptive Z chromosome evolution in two divergent lepidopteran lineages. *Evolution*, *76*(2), 332–345. https://doi.org/10.1111/evo.14341

Morales, H. E., Pavlova, A., Amos, N., Major, R., Kilian, A., Greening, C., & Sunnucks, P. (2018). Concordant divergence of mitogenomes and a mitonuclear gene cluster in bird lineages inhabiting different climates. *Nature Ecology & Evolution*, *2*(8), 1258–1267. https://doi.org/10.1038/s41559-018-0606-3

Moritz, C., Fujita, M. K., Rosauer, D., Agudo, R., Bourke, G., Doughty, P., Palmer, R., Pepper, M., Potter, S., Pratt, R., Scott, M., Tonione, M., & Donnellan, S. (2016). Multilocus phylogeography reveals nested endemism in a gecko across the monsoonal tropics of Australia. *Molecular Ecology*, *25*(6), 1354–1366. https://doi.org/10.1111/mec.13511

Nam, K., & Ellegren, H. (2008). The chicken (*Gallus gallus*) Z chromosome contains at least three nonlinear evolutionary strata. *Genetics*, *180*(2), 1131–1136. https://doi.org/10.1534/genetics.108.090324

Nielsen, R., Akey, J. M., Jakobsson, M., Pritchard, J. K., Tishkoff, S., & Willerslev, E. (2017). Tracing the peopling of the world through genomics. *Nature*, *541*(7637), 302–310. https://doi.org/10.1038/nature21347

Norman, J. A., Rheindt, F. E., Rowe, D. L., & Christidis, L. (2007). Speciation dynamics in the Australo-Papuan Meliphaga honeyeaters. *Molecular Phylogenetics and Evolution*, *42*(1), 80–91. https://doi.org/10.1016/j.ympev.2006.05.032

Oliveros, C. H., Field, D. J., Ksepka, D. T., Barker, F. K., Aleixo, A., Andersen, M. J., Alström, P., Benz, B. W., Braun, E. L., Braun, M. J., Bravo, G. A., Brumfield, R. T., Chesser, R. T., Claramunt, S., Cracraft, J., Cuervo, A. M., Derryberry, E. P., Glenn, T. C., Harvey, M. G., … Faircloth, B. C. (2019). Earth history and the passerine superradiation. *Proceedings of the National Academy of Sciences of the United States of America*, *116*(16), 7916–7925. https://doi.org/10.1073/pnas.1813206116

Otto, S. P., Pannell, J. R., Peichel, C. L., Ashman, T.-L., Charlesworth, D., Chippindale, A. K., Delph, L. F., Guerrero, R. F., Scarpino, S. V., & McAllister, B. F. (2011). About PAR: The distinct evolutionary dynamics of the pseudoautosomal region. *Trends in Genetics*, *27*(9), 358–367. https://doi.org/10.1016/j.tig.2011.05.001

Pala, I., Naurin, S., Stervander, M., Hasselquist, D., Bensch, S., & Hansson, B. (2012). Evidence of a neo-sex chromosome in birds. *Heredity*, *108*(3), 264–272. https://doi.org/10.1038/hdy.2011.70

Palmer, D. H., Rogers, T. F., Dean, R., & Wright, A. E. (2019). How to identify sex chromosomes and their turnover. *Molecular Ecology*, *28*(21), 4709–4724. https://doi.org/10.1111/mec.15245

Paradis, E., Claude, J., & Strimmer, K. (2004). APE: Analyses of phylogenetics and evolution in R language. *Bioinformatics*, *20*(2), 289–290. https://doi.org/10.1093/bioinformatics/btg412

Peñalba, J. V., Deng, Y., Fang, Q., Joseph, L., Moritz, C., & Cockburn, A. (2020). Genome of an iconic Australian bird: High-quality assembly and linkage map of the superb fairy-wren (*Malurus cyaneus*). *Molecular Ecology Resources*, *20*(2), 560–578. https://doi.org/10.1111/1755-0998.13124

Peñalba, J. V., Joseph, L., & Moritz, C. (2019). Current geography masks dynamic history of gene flow during speciation in northern Australian birds. *Molecular Ecology*, *28*(3), 630–643. https://doi.org/10.1111/mec.14978

Peñalba, J. V., Mason, I. J., Schodde, R., Moritz, C., & Joseph, L. (2017). Characterizing divergence through three adjacent Australian avian transition zones. *Journal of Biogeography*, *44*(10), 2247–2258. https://doi.org/10.1111/jbi.13048

Peona, V., Blom, M. P. K., Xu, L., Burri, R., Sullivan, S., Bunikis, I., Liachko, I., Haryoko, T., Jønsson, K. A., Zhou, Q., Irestedt, M., & Suh, A. (2021). Identifying the causes and consequences of assembly gaps using a multiplatform genome assembly of a bird-of-paradise. *Molecular Ecology Resources*, *21*(1), 263–286. https://doi.org/10.1111/1755-0998.13252

Pepper, M., Hamilton, D. G., Merkling, T., Svedin, N., Cser, B., Catullo, R. A., Pryke, S. R., & Keogh, J. S. (2017). Phylogeographic structure across one of the largest intact tropical savannahs: Molecular and morphological analysis of Australia's iconic frilled lizard *Chlamydosaurus kingii*. *Molecular Phylogenetics and Evolution*, *106*, 217–227. https://doi.org/10.1016/j.ympev.2016.09.002

Petkova, D., Novembre, J., & Stephens, M. (2016). Visualizing spatial population structure with estimated effective migration surfaces. *Nature Genetics*, *48*(1), 94–100. https://doi.org/10.1038/ng.3464

Patterson, N., Moorjani, P., Luo, Y., Mallick, S., Rohland, N., Zhan, Y., Genschoreck, T., Webster, T., & Reich, D. (2012). Ancient admixture in human history. *Genetics*, *192*(3), 1065–1093. https://doi.org/10.1534/genetics.112.145037

Ponnikas, S., Sigeman, H., Lundberg, M., & Hansson, B. (2022). Extreme variation in recombination rate and genetic diversity along the Sylvioidea neo-sex chromosome. *Molecular Ecology*, *31*(13), 3566–3583. https://doi.org/10.1111/mec.16532

Pickrell, J. K., & Pritchard, J. K. (2012). Inference of population splits and mixtures from genome-wide allele frequency data. *PLoS Genetics*, *8*(11), e1002967. https://doi.org/10.1371/journal.pgen.1002967

Pool, J. E., & Nielsen, R. (2007). Population size changes reshape genomic patterns of diversity. *Evolution*, *61*(12), 3001–3006. https://doi.org/10.1111/j.1558-5646.2007.00238.x

Ralls, K., Ballou, J. D., Dudash, M. R., Eldridge, M. D. B., Fenster, C. B., Lacy, R. C., Sunnucks, P., & Frankham, R. (2018). Call for a paradigm shift in the genetic management of fragmented populations. *Conservation Letters*, *11*(2), e12412. https://doi.org/10.1111/conl.12412

Ravinet, M., Kume, M., Ishikawa, A., & Kitano, J. (2021). Patterns of genomic divergence and introgression between Japanese stickleback species with overlapping breeding habitats. *Journal of Evolutionary Biology*, *34*(1), 114–127. https://doi.org/10.1111/jeb.13664

Rech, G. E., Radío, S., Guirao-Rico, S., Aguilera, L., Horvath, V., Green, L., Lindstadt, H., Jamilloux, V., Quesneville, H., & González, J. (2022). Population-scale long-read sequencing uncovers transposable elements associated with gene expression variation and adaptive signatures in Drosophila. *Nature Communications*, *13*(1), 1948. https://doi.org/10.1038/s41467-022-29518-8

Reeves, J. M., Chivas, A. R., Garcia, A., & De Deckker, P. (2007). Palaeoenvironmental change in the Gulf of Carpentaria (Australia) since the last interglacial based on Ostracoda. *Palaeogeography, Palaeoclimatology, Palaeoecology*, *246*(2–4), 163–187. https://doi.org/10.1016/j.palaeo.2006.09.012

Reeves, J. M., Chivas, A. R., García, A., Holt, S., Couapel, M. J. J., Jones, B. G., Cendón, D. I., & Fink, D. (2008). The sedimentary record of palaeoenvironments and sea-level change in the Gulf of Carpentaria, Australia, through the last glacial cycle. *Quaternary International*, *183*(1), 3–22. https://doi.org/10.1016/j.quaint.2007.11.019

Rhie, A., McCarthy, S. A., Fedrigo, O., Damas, J., Formenti, G., Koren, S., Uliano-Silva, M., Chow, W., Fungtammasan, A., Kim, J., Lee, C., Ko, B. J., Chaisson, M., Gedman, G. L., Cantin, L. J., Thibaud-Nissen, F., Haggerty, L., Bista, I., Smith, M., … Jarvis, E. D. (2021). Towards complete and error-free genome assemblies of all vertebrate species. *Nature*, *592*(7856), 737–746. https://doi.org/10.1038/s41586-021-03451-0

Robledo-Ruiz, D. A., Gan, H. M., Kaur, P., Dudchenko, O., Weisz, D., Khan, R., Lieberman Aiden, E., Osipova, E., Hiller, M., Morales, H. E., Magrath, M. J. L., Clarke, R. H., Sunnucks, P., & Pavlova, A. (2022). Chromosome-length genome assembly and linkage map of a critically endangered Australian bird: The helmeted honeyeater. *GigaScience*, *11*, https://doi.org/10.1093/gigascience/giac025

Saitou, N., & Nei, M. (1987). The neighbor-joining method: A new method for reconstructing phylogenetic trees. *Molecular Biology and Evolution*, *4*(4), 406–425. https://doi.org/10.1093/oxfordjournals.molbev.a040454

Sardell, J. (2016). *Evolutionary consequences of recent secondary contact between Myzomela honeyeaters* [Ph.D. Thesis]. University of Miami. https://scholarship.miami.edu/esploro/outputs/991031447092302976

Schodde, R., & Mason, I. J. (1999). *Directory of Australian birds: Passerines*. CSIRO publishing.

Shakya, S. B., Wang-Claypool, C. Y., Cicero, C., Bowie, R. C. K., & Mason, N. A. (2022). Neo-sex chromosome evolution and phenotypic differentiation across an elevational gradient in horned larks (*Eremophila alpestris*). *Molecular Ecology*, *31*(6), 1783–1799. https://doi.org/10.1111/mec.16357

Sigeman, H. (2021). *Evolution of sex chromosomes in Sylvioidea songbirds* [Dissertation]. Lund University.

Sigeman, H., Ponnikas, S., Chauhan, P., Dierickx, E., Brooke, M. L., & Hansson, B. (2019). Repeated sex chromosome evolution in vertebrates supported by expanded avian sex chromosomes. *Proceedings of the Royal Society B: Biological Sciences*, *286*(1916), 20192051. https://doi.org/10.1098/rspb.2019.2051

Sigeman, H., Ponnikas, S., & Hansson, B. (2020). Whole-genome analysis across 10 songbird families within Sylvioidea reveals a novel autosome–sex chromosome fusion. *Biology Letters*, *16*(4), 20200082. https://doi.org/10.1098/rsbl.2020.0082

Sigeman, H., Strandh, M., Proux-Wéra, E., Kutschera, V. E., Ponnikas, S., Zhang, H., Lundberg, M., Soler, L., Bunikis, I., Tarka, M., Hasselquist, D., Nystedt, B., Westerdahl, H., & Hansson, B. (2021). Avian neo-sex chromosomes reveal dynamics of recombination suppression and W degeneration. *Molecular Biology and Evolution*, *38*, 5275–5291. https://doi.org/10.1093/molbev/msab277

Simão, F. A., Waterhouse, R. M., Ioannidis, P., Kriventseva, E. V., & Zdobnov, E. M. (2015). BUSCO: Assessing genome assembly and annotation completeness with single-copy orthologs. *Bioinformatics*, *31*(19), 3210–3212. https://doi.org/10.1093/bioinformatics/btv351

Smeds, L., Kawakami, T., Burri, R., Bolivar, P., Husby, A., Qvarnström, A., Uebbing, S., & Ellegren, H. (2014). Genomic identification and characterization of the pseudoautosomal region in highly differentiated avian sex chromosomes. *Nature Communications*, *5*, 5448.

Soulé, M. (1973). The epistasis cycle: A theory of marginal populations. *Annual Review of Ecology and Systematics*, *4*(1), 165–187. https://doi.org/10.1146/annurev.es.04.110173.001121

Stange, M., Sánchez-Villagra, M. R., Salzburger, W., & Matschiner, M. (2018). Bayesian divergence-time estimation with genome-wide single-nucleotide polymorphism data of sea catfishes (Ariidae) supports Miocene closure of the Panamanian isthmus. *Systematic Biology*, *67*(4), 681–699. https://doi.org/10.1093/sysbio/syy006

Stimpson, K. M., Matheny, J. E., & Sullivan, B. A. (2012). Dicentric chromosomes: Unique models to study centromere function and inactivation. *Chromosome Research*, *20*(5), 595–605. https://doi.org/10.1007/s10577-012-9302-3

Stryjewski, K. F., & Sorenson, M. D. (2017). Mosaic genome evolution in a recent and rapid avian radiation. *Nature Ecology & Evolution*, *1*(12), 1912–1922. https://doi.org/10.1038/s41559-017-0364-7

Tajima, F. (1989). The effect of change in population size on DNA polymorphism. *Genetics*, *123*(3), 597–601. https://doi.org/10.1093/genetics/123.3.597

Talla, V., Pierce, A. A., Adams, K. L., de Man, T. J. B., Nallu, S., Villablanca, F. X., Kronforst, M. R., & de Roode, J. C. (2020). Genomic evidence for gene flow between monarchs with divergent migratory phenotypes and flight performance. *Molecular Ecology*, *29*(14), 2567–2582. https://doi.org/10.1111/mec.15508

Toon, A., Drew, A., Mason, I. J., Hughes, J. M., & Joseph, L. (2017). Relationships of the New Guinean subspecies, *Gymnorhina tibicen papuana*, of the Australian Magpie: An assessment from DNA sequence data. *Emu - Austral Ornithology*, *117*(4), 305–315. https://doi.org/10.1080/01584197.2017.1324249

Toon, A., Hughes, J. M., & Joseph, L. (2010). Multilocus analysis of honeyeaters (Aves: Meliphagidae) highlights spatio-temporal heterogeneity in the influence of biogeographic barriers in the Australian monsoonal zone. *Molecular Ecology*, *19*(14), 2980–2994. https://doi.org/10.1111/j.1365-294X.2010.04730.x

Webster, T. H., Couse, M., Grande, B. M., Karlins, E., Phung, T. N., Richmond, P. A., Whitford, W., & Wilson, M. A. (2019). Identifying, understanding, and correcting technical artifacts on the sex chromosomes in next-generation sequencing data. *GigaScience*, *8*(7), 1–11. https://doi.org/10.1093/gigascience/giz074

Weissensteiner, M. H., Bunikis, I., Catalán, A., Francoijs, K.-J., Knief, U., Heim, W., Peona, V., Pophaly, S. D., Sedlazeck, F. J., Suh, A., Warmuth, V. M., & Wolf, J. B. W. (2020). Discovery and population genomics of structural variation in a songbird genus. *Nature Communications*, *11*(1), 3403. https://doi.org/10.1038/s41467-020-17195-4

Williams, D. J., O'shea, M., Daguerre, R. L., Pook, C. E., Wüster, W., Hayden, C. J., Mcvay, J. D., Paiva, O., Matainaho, T., Winkel, K. D., & Austin, C. C. (2008). Origin of the eastern brownsnake, *Pseudonaja textilis* (Dumeril, Bibron and Dumeril) (Serpentes: Elapidae: Hydrophiinae) in New Guinea: Evidence of multiple dispersals from Australia, and comments on the status of *Pseudonaja textilis pughi* Hoser 2003. *Zootaxa*, *1703*(1), 47–61. https://doi.org/10.11646/zootaxa.1703.1.3

Wilson Sayres, M. A. (2018). Genetic diversity on the sex chromosomes. *Genome Biology and Evolution*, *10*(4), 1064–1078. https://doi.org/10.1093/gbe/evy039

Wright, A. E., Harrison, P. W., Montgomery, S. H., Pointer, M. A., & Mank, J. E. (2014). Independent stratum formation on the avian sex chromosomes reveals inter-chromosomal gene conversion and predominance of purifying selection on the W chromosome. *Evolution*, *68*(11), 3281–3295. https://doi.org/10.1111/evo.12493

Wüster, W., Dumbrell, A. J., Hay, C., Pook, C. E., Williams, D. J., & Fry, B. G. (2005). Snakes across the strait: Trans-Torresian phylogeographic relationships in three genera of Australasian snakes (Serpentes: Elapidae: Acanthophis, Oxyuranus, and Pseudechis). *Molecular Phylogenetics and Evolution*, *34*(1), 1–14. https://doi.org/10.1016/j.ympev.2004.08.018

Yamaguchi, R., & Iwasa, Y. (2017). Parapatric speciation in three islands: Dynamics of geographical configuration of allele sharing. *Royal Society Open Science*, *4*(2), 160819. https://doi.org/10.1098/rsos.160819

Yokoyama, Y., Purcell, A., Lambeck, K., & Johnston, P. (2001). Shoreline reconstruction around Australia during the last glacial maximum and late glacial stage. *Quaternary International*, *83–85*, 9–18. https://doi.org/10.1016/S1040-6182(01)00028-3

Yoshida, K., & Kitano, J. (2012). The contribution of female meiotic drive to the evolution of neo-sex chromosomes. *Evolution*, *66*(10), 3198–3208. https://doi.org/10.1111/j.1558-5646.2012.01681.x

Yoshida, K., Makino, T., & Kitano, J. (2017). Accumulation of deleterious mutations on the neo-Y chromosome of Japan Sea stickleback (*Gasterosteus nipponicus*). *Journal of Heredity*, *108*(1), 63–68. https://doi.org/10.1093/jhered/esw054

SUPPORTING INFORMATION

Additional supporting information can be found online in the Supporting Information section at the end of this article.

How to cite this article: Burley, J. T., Orzechowski, S. C. M., Sin, S. Y. W., & Edwards, S. V. (2022). Whole-genome phylogeography of the blue-faced honeyeater (*Entomyzon cyanotis*) and discovery and characterization of a neo-Z chromosome. *Molecular Ecology*, *00*, 1–23. https://doi.org/10.1111/mec.16604